NTNU – Trondheim
Norwegian University of
Science and Technology

GNSS/INS Integration in Urban Areas

Shafiq Muhammad

Electronics System Design and Innovation
Submission date: April 2014
Supervisor: Jon Glenn Omholt Gjevestad, IET

Norwegian University of Science and Technology
Department of Electronics and Telecommunications

Abstract

The Satellite based navigation systems are often integrated with inertial navigation systems in order to provide greater accuracy and reliability in the position and velocity parameters. For this purpose high quality inertial sensors are used which can provide real-time navigation at centimeter level. Price, size and weight of traditional INS has been a problem which has been solved successfully by the use of Micro Electro Mechanical Sensors (MEMS). The problem with the MEMS technology is the large error which grows rapidly and degrade the performance of the navigation system. Different methods are used to calculate the error coefficients (not implemented in this study work) which are further used in a kalman filter in order to enhance the performance of the system. Thus a kalman filter has been introduced to perform the data fusion algorithms. Kalman filtering is a recursive technique used to optimize the state vector of the estimates and it efficiently provides the navigation estimates of a dynamic system. All the navigation data used in this thesis work has been provided by my supervisor, professor Jon Glenn Gjevestad (UMB). A real-time system has been tested in the urban areas for different scenarios. Kalman filter approach with loose integration has been implemented. A comparison of the filtered solution with the reference positions has been made by introducing a 2D horizontal position error in order to analyze the position accuracy. In the end some recommendations on future work are courted.

Acknowledgements

First of all, I would like to express my sincere gratitude to my supervisor, professor Jon Glenn Gjevestad, for all type of help he gave me during my thesis time. He is working as a professor at Department of Mathematical Sciences and Technology (NMBU) and teaching a course (Navigation Systems) at NTNU. He helped me a lot to understand the orientation of the problem conceptually and systematically.

Secondly, I would like to express special thanks to my family, especially my dear parents, brothers, sisters, my wife, kids and friends who have always great love and prayers for me. These facts always boost up my motivations and make me energetic to work hard in order to achieve the objective.

April 3, 2014, NTNU
Muhammad Shafiq

Dedication
TO
the brave people of Thar Desert (Pakistan).

Table of Contents

List of Figures

List of Tables

Chapter 1

Introduction

The GPS has played a vital role in the human life . The usage of GPS receivers has become very common in every days life. The need of GPS cant be denied specially when it concerns the field of navigation, weather forecasting, communication networks, tectonic movements, reference frames and time and frequency transforms. Despite of these important applications there are many other applications where the GPS systems are used. The accuracy of any GPS receiver depends on many factors such as operational environments, the quality of the IMU and the integration method implemented. For example, system performance is directly related to the signal quality which is independent of local environments. But in many investigated areas, the accuracy varies a lot. It may vary 10 cm over one second or decimeter-level over 20 seconds [18]. Particularly, it is quite difficult to meet the accuracy requirements in the urban areas where the GPS signal may be blocked by the high buildings or may be reflected and cause multipath [19]. Multipath causes strong effects on the signal quality and the measurement errors are produced. Thus actually only the GPS is not enough to meet the accuracy requirements especially when it concerns the navigation in urban areas. To enhance the accuracy, GPS has to be combined with some other systems like INS (Inertial Navigation System). An INS utilizes the inertial sensors and the output data of these sensors is combined to get better estimates. Usually in the high accuracy applications GPS is integrated with high-end INS. It has already been proven in various investigations that GPS/INS integration provides more accuracy and reliability than GPS or INS alone. Dynamic models and measurements are used to make the quality control effective. Then the detection and identification of the errors both in the dynamic and measurement model is done by applying the algorithms such as RAIM (Receiver Autonomous Integrity Monitoring) and eRAIM (Extended Receiver Autonomous Integrity Monitoring [20]. The kalman filter is very common to use for this pur-

pose. It simply extracts the required information and ignoring the rest. The state parameters are estimated by the method of least-squares which are further used to develop the above mentioned algorithms (RAIM, eRAIM).

1.1 Background

Filtering is a common technique when analyzing the random signals. There are various types of filters and techniques used for filtering. Optimal filter problems have successfully been solved by using wiener filters both in continuous and discrete case by utilizing the weight function. It determines the information about the weights to be assigned to the past state values which will then determine the present state value. But the wiener filter solution will not be suitable for the complex and multi-task problems [3, ch5]. An alternative solution was published by Rudolf Emil Kalman in 1960 which provides a recursive solution to the discrete signals on the basis of state space techniques. Scientists and engineers found very quickly that the algorithm was very practical, especially in case of space related applications and in the field of navigation. Many of the problems which were impossible by wiener filtering could now be solved by kalman filtering. It became a milestone and revolutionary step in the field of signal processing. Since then it has been a popular topic in extensive research areas. Especially the vector modeling and noisy data handling by recursive algorithms are two main features of the Kalman filter [21]. The filter is a powerful tool used to estimate the past, present and future state values as well [22].

1.2 Main goal

Satellite based navigation systems have become very common and popular in our lives today. Especially the traffic surveillance has a wide use of these systems. The modern vehicles come with integrated GPS (Global Positioning System) in these days. But only using the GPS may not be enough when it concerns the high accuracy navigation applications. Especially the navigation accuracy is very poor in the urban areas. Therefore GPS is integrated usually with inertial navigation systems (INS) in order to enhance the accuracy and reliability. A Kalman filter provides the basis for this type of applications. It predicts the INS observations and corrects them with the GPS measurements [22]. So our focus will be on the following three objectives through this study work.

- The first one is to integrate both GPS and IMU data files and analyze the performance of the both systems.

- The second one is to develop and implement a kalman filter in Matlab (Matrix Laboratory) for GPS/IMU integration for low-end sensors.
- The third one is to analyze the integrated solution performance with and without kalman filter implementation.

1.3 Thesis outline

Chapter 2 briefly explained the system architecture of the Global Positioning System (GPS), GPS observables, differential GPS and typical error sources involved. Inertial Navigation System (INS) along with inertial sensors has been explained briefly. In the last part of the chapter, MEMS based inertial technology has been explained briefly. Chapter 3 defines different reference frames and their properties involved in both systems. Direction Cosine Matrices (DCM) are introduced in order to make the transformations possible between the different frames of reference. Chapter 4 describes the system kinematics of INS with respect to different frames of reference, observation equations for inertial sensors, and common methods for attitude representation of a vehicle. Chapter 5 focuses mainly on two commonly used integration strategies and their implementation methods in the first section. In the second section, discrete kalman filter algorithm together with its dynamic and measurement models has been described. Numerical calculation for matrices involved in the kalman filter design, has also been shown. Chapter 6 discusses the planed vehicle mission, system hardware setup, the inertial sensors used for the vehicle mission and represents the results and analysis. . Chapter 7 gives a summary of the thesis and conclusions which have been made in the light of the results and analysis represented in chapter 6.

Chapter 2

GPS/INS Architecture

A satellite navigation system is capable of providing the autonomous geo-spatial positioning all around the Earth. This position (longitude, latitude, altitude), within few meters of accuracy, can be determined by using small electronic receivers. Such a system may be called as Global Navigation Satellite System (GNSS). Currently, the United States NAVSTAR Global Positioning System (GPS) and Russian Globalnaya Navigatsionnaya Sputnikovaya Sistema (GLONASS) operated by Russian Aerospace Defence Forces, are the only examples of GNSS. The Chinese regional navigation system BEIDOU is being expanded to a global navigation system Compass and European Unions global navigation system GALILEO are expected to start their operations by end of 2020 [1]. In this study work, we have chosen the United States GPS to integrate with INS, therefore our focus will be on GPS throughout the thesis. A comparison among accuracy levels of different radio navigation systems is shown below in the Figure **??**.

There are many types of navigation systems which can be integrated with GPS, but because of the complementary characteristics of the GPS and INS, INS has been the most attractive one in many investigations. Inertial Navigation System (INS) has the capability to provide the data for the short-term changes in the vehicle position even if signal is being blocked by some reasons [4]. Before we discuss GPS/INS system structure as a whole, we will first review the characteristics and limitations of the each system individually. There are many types of navigation systems which can be integrated with GPS, but because of the complementary characteristics of the GPS and INS, INS has been the most attractive one in many investigations. Inertial Navigation System (INS) has the capability to provide the data for the short-term changes in the vehicle position even if signal is being blocked by some reasons [23]. Before we discuss GPS/INS system structure as a whole, we will first review the characteristics and limitations of the each

system individually.

2.1 GPS: An Overview of the system

The Global Positioning System (GPS) utility is owned by USA. The system is capable of providing continuous and highly accurate position, navigation and timing (PNT) services. It uses NAVSTAR (NAVigation Satellite Timing And Ranging) utility which has 24 operational satellites [24]. Starting with brief history of GPS, this section provides an overview of the system architecture, error sources, signal characteristics and measurements.

2.1.1 Main Objective and Brief History

Since the clocks on the earth are affected by the gravitational force, so the idea behind the project was to take the advantage of using atomic clocks in the navigation satellites in order to enhance the accuracy in the time measurements [4]. In the beginning, the GPS has been used as a military system. It was developed by the U.S. Department of Defense (DoD) in order to facilitate the U.S. military by accurate measurements of PVT (Position, velocity and time) parameters in a common reference system around the globe [25]. U.S. Department of Defense decided to offer the civilians only the Standard Positioning Service (SPS) capability which was intentionally corrupted by controlled errors to reduce the accuracy of the system. The technique used was called Selective Availability (SA). On the other side, Precise Positioning Service (PPS) which was the full capability of the system, was only accessible by the U.S. Military. Here the transmitted signal was encrypted for Military users which could possibly be decrypted by the authorities by using proper keys. The technique was called Anti-Spoofing (AS) and it was intentionally used because of the national security issues. The Korean airline accident brought the intension of authorities to review the U.S policy about the worldwide use of GPS. Soviet air defense shot down a Korean civil airline in sep.1, 1983 at Sakhalin Peninsula. After that incident President Reagan ordered that the GPS service will be available for the civilian users as well. Hence the Initial Operative Capability (IOC) was accessible by the civilian users in the year of 1993. In 2 May, 2000, the President Bill Clinton ordered to end the Selective Availability (SA) and in 2004 President Bush announced the free of charge continuity of the GPS service as a global navigation service for the civilians [4] .

2.2 System Architecture

Currently the GPS is consisting of the following three main segments as shown in the figure below.

- Space Segment (SS)
- Control Segment (CS)
- User Segment (US)

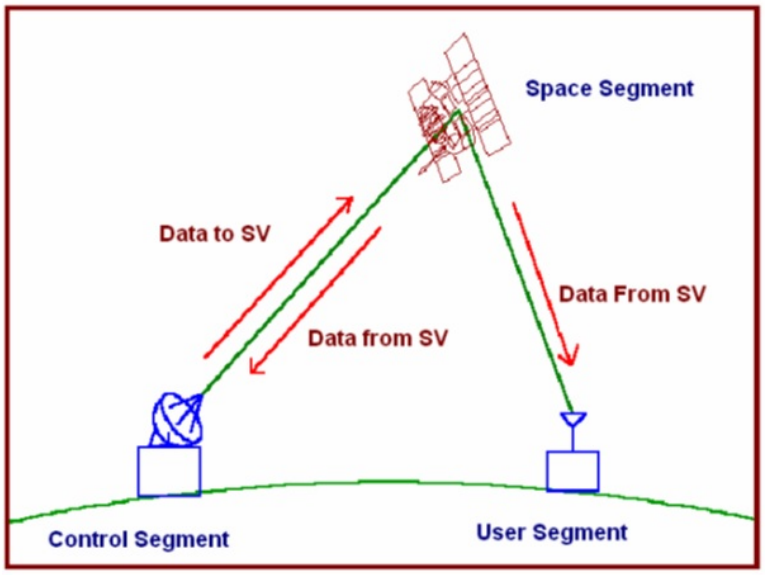

Figure 2.1: GPS segments representation diagram [2]

The Pseudo-Random Noise (PRN) code for each satellite vehicle (SV) is unique which helps the receiver to easily identify a satellite vehicle. The space segment deals directly with the satellites and the control segment deals with the operation of the satellite. U.S Department of Defense is taking care of both of these segments. The user segment relates to the military and civil sector.

2.2.1 The space segment

The space segment is composed of satellite constellation which is transmitting the GPS signals to the GPS receivers on the Earth. The U.S. Air Force is managing the constellation and ensuring the signal availability for the users. There have been 31 operational satellites with 3 or 4 additional satellites which could be activated

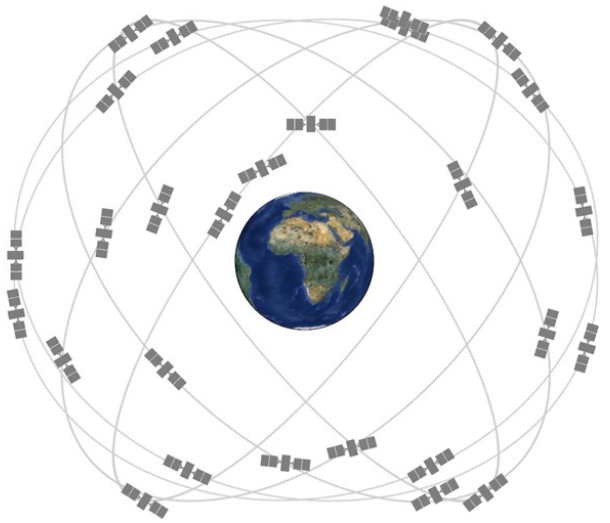

Figure 2.2: GPS Expandable-24 Satellite Configuration [3]

if needed. The U.S. Air Force added three more satellites to the constellation in June 2011, without changing the core constellation. This extension may increase the GPS performance [3]. The space segment consists of 24 navigation satellites orbiting in 6 orbital planes (almost circular). Inclination angle is 55 and the orbital radius is about 26650 km with 11 hours and 58 minutes orbital period. Repetition rate is one sidereal day [16]. These GPS satellites are orbiting in medium Earth orbit (MEO) at an altitude of 20,200 km. The satellites make two rotations around the Earth every day.

2.2.2 The Control Segment

U.S. Air Force monitoring stations, operated by National Geospatial-Intelligence Agency (NGA), are tracking the navigation satellites around the world by using ground facilities. The Master Control Station, located in Colorado Springs, commands the satellite operational functions like orbit corrections, general satellite health, GPS time, prediction of ephemerides and clock parameters, navigation message updates etc [25]. Usually there are three to four atomic clocks on a GPS satellite. These clocks are operating at fundamental L-band frequency which is 10.23 MHz. The control signals are sent to the satellite clocks to reduce the difference between the clocks. GPS has its own time reference which is called GPS time (GPST) and the offset between GPST and UTC is being tracked all the time [25].

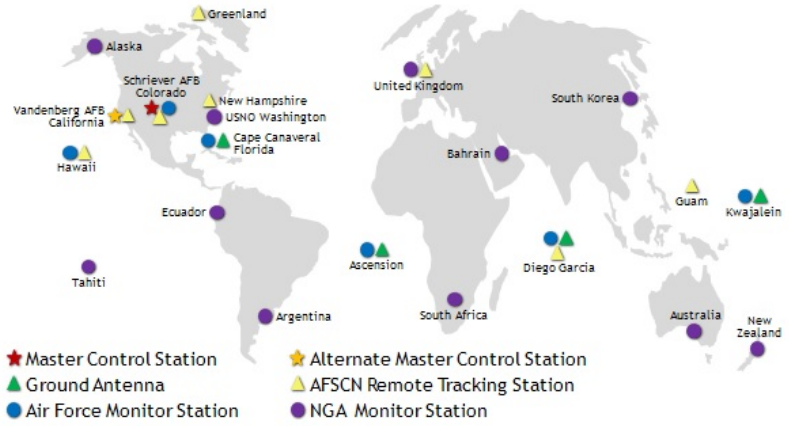

Figure 2.3: GPS Control Segment Ground Facilites [3]

2.2.3 The User Segment

The user segment is simply the GPS receiver used to detect the signal transmitted by a GPS satellite. There are several different types of receivers. The accuracy of a GPS is highly dependent on the clock used in the receiver. A GPS receiver actually measures the distance between the GPS satellite and itself by measuring the time slot when the signal was transmitted by the GPS satellite and detected on Earth by the GPS receiver. Since the signal is travelling with the speed of light, this time slot is then multiplied by the travelling speed of the signal and hence the distance is calculated. The detected microwave signal is carrying the information about the satellite coordinates. A GPS receiver normally calculates the distance to 3 or 4 satellites and then by using trilateration technique, it calculates its own coordinates. Trilateration is a mathematical technique which measures the distances by using the geometry of spheres and triangles in order to determine the absolute or relative positions.

2.3 Navigation Signal

A GPS satellite transmits two radio frequencies at 50 bits/sec with a bit duration of 20 ms in the L-band which is called a Navigation Message. These two frequencies are called L1 (1575.42 MHz) and L2 (1227.60 MHz) [25]. The scheme used for the modulation of the signal is Code Division Multiple Access (CDMA). Three components of the GPS signal are carrier, Ranging code and navigation data. A carrier is a radio frequency either L1 or L2. Ranging codes are Pseudo-Random

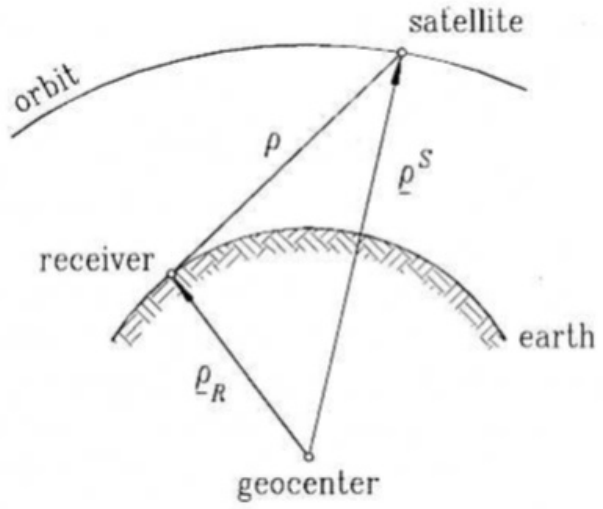

Figure 2.4: Receiver/Satellite Geometry [4]

Noise (PRN) codes or sequences which are used to measure the ranges. This sequence looks like noise but it is generated by the shift register. PRN codes are of two types which are Coarse/Acquisition code (C/A code, L1) and Precise code (P code, L1, L2). The navigation data consists of ephemeris (position and velocity of the satellite), status of the satellite, clock parameters and an almanac which consists of status of the satellite in the orbit. The transmission time for a complete almanac is 12.5 minutes. The satellites position in the orbit (ephemeris) and clock parameters are sent every 30 seconds [25]. These signal characteristics can be used to determine the following measurements which are explained in details in the following section.

- *Pseudurange measurements*
  Since the origin of the pseudorange measurements are the PRN code sequences, they are dependent on the code and frequency of the sequence.

- *Carrier phase measurements*
  The GPS receiver identifies a satellite by measuring the phase of the received carrier and then the distance to the satellite is measured.

- *Doppler measurements*
  The Doppler effect which is caused by the relative motion of the satellite

and the receiver, can be measured by differentiating the carrier phase measurements [18].

2.4 GPS: Observation Equations

Most of the present technology GPS receivers are capable of providing the following three types of measurements from a navigation signal.

- Pseudorange/code phase measurements
- Carrier phase measurements
- Doppler measurements

2.4.1 Pseudo-range Measurements

PRN codes are used to identify the satellites and to access the information from the satellite to the ground. Pseudo-ranges are derived from these codes. A pseudo-range is basically a measure of the distance between the satellite antenna and the receiver antenna (difference between the signal transmission and reception time). They are calculated by multiplying these time differences by the speed of light in vacuum as follows

$$\rho = c.\delta t \tag{2.1}$$

where,
ρ denotes the pseudo-range,
c is the speed of light in vacuum,
δt is the time difference (transit time).

The transmitted signal is marked with the time stamp by a clock on board but the correlation of the received signal and the replica generated by the receiver gives the reception time. Hence the receiver and the satellite have their own independent times which need to be synchronized. A time shift of I ms as a biased is used for this purpose [25]. The pseudo-ranges for a satellite and receiver are written by using the Pythagoras Theorem.

$$\rho_r^s = (X^s - X_r)^2 + (Y^s - Y_r)^2 + (Z^s - Z_r)^2, \tag{2.2}$$

where X^s, Y^s, Z^s are satellite coordinates and X_R, Y_R, Z_R are receiver coordinates.
These differences are non-linear since they are geometrical distances between the satellite and the receiver. They are linearized by using the method of least-squares

adjustment. Hence based on the code phase measurements/pseudo-range measurements, the observation equation for GPS can be written as

$$R = \rho + c(\delta t_R - \delta t^s) + I_R + T_R + \varepsilon_R \quad \text{(in meters)}, \tag{2.3}$$

Where,
R denotes the noisy and biased measurements of ρ (meters).
ρ denotes the true ranges between the satellite antenna and the receiver antenna at t^s, t_R respectively (meters)
c speed of light in vacuum (m/sec)
δt^s satellite clock bias
δt_R receiver clock bias
I_R ionospheric delay in the signal (meter)
T_R tropospheric delay in the signal (meter)
ϵ_R denote the errors in the model and measurements and the effects which are not included in the model.

2.4.2 Carrier Phase Measurements

The phase of the incoming carrier may be used to measure the ranges to the satellite which is more precise than the code phase. So these are basically the phase differences between the received carrier and the carrier generated by the receiver. The phase of a cycle can be measured exactly but there is no information about the number of complete and fractional cycles from the satellite to the receiver and this fact introduces the integer ambiguity (IA). The sum of cycles (complete and fractional) is multiplied by the carrier wavelength after resolving the integer ambiguity [10] as shown below.

$$\rho = (N + \varphi).\lambda \tag{2.4}$$

Where N and φ denote the complete and fractional cycles respectively and λ denotes the carrier wavelength. The equation can be rewritten, by considering the measurement errors, ionospheric and tropospheric delays and clock biases, in the following form

$$\varphi = \frac{1}{\lambda}(\rho + c\delta t_R - c\delta t^s - I_\varphi + T_\varphi) + \lambda N + \varepsilon_\varphi \tag{2.5}$$

The units can be converted into meters by multiplying the above equation by the wavelength

$$\phi = \rho + c\delta t_R - c\delta t^s - I_\varphi + T_\varphi + \lambda N + \varepsilon_\phi \tag{2.6}$$

where,
ϕ denotes the carrier phase measurements

$I_\varepsilon + T_\varepsilon$ represents ionospheric and tropospheric propagation delays respectively (meters)
N represent ambiguous number of cycles
ε_φ denote the errors in the measurements (cycles)
ε_ϕ noise
$\varepsilon_\phi \ll \varepsilon_R$

2.4.3 Doppler measurements

The relative motion of the satellite and the receiver causes a shift in the frequency of the electromagnetic signal. This well-known phenomenon is known as the Doppler effect. Some of the GPS receivers use Doppler frequency in order to compute the velocity of the user [10]. The Doppler shift is computed by the following formula

$$f_d = -\frac{\dot{r}}{\lambda} \tag{2.7}$$

Where f_d denotes the Doppler shift,$\dot{r}$ line-of-sight range rate and λ is the wavelength.

2.5 Differential GPS (DGPS)

Another more precise technique used for navigation is known as differential GPS. Differential GPS acquired two GPS receivers, one with known position which is used as a reference station and the second one is mounted on the vehicle which measures its position relative to the reference station.

There are further two types of differential GPS depending on weather we are using pseudorange measurements or carrier phase measurements from the navigation signal.

- DGPS
- Relative Positioning

2.5.1 DGPS

The technique is simply known as DGPS when the pseudorange measurements are used in the differential GPS. This method was implemented to eliminate the Selective Availability (SA) and thus the accuracy was increased by a factor of ten. Function of the DGPS is to reduce the atmospheric error [26].

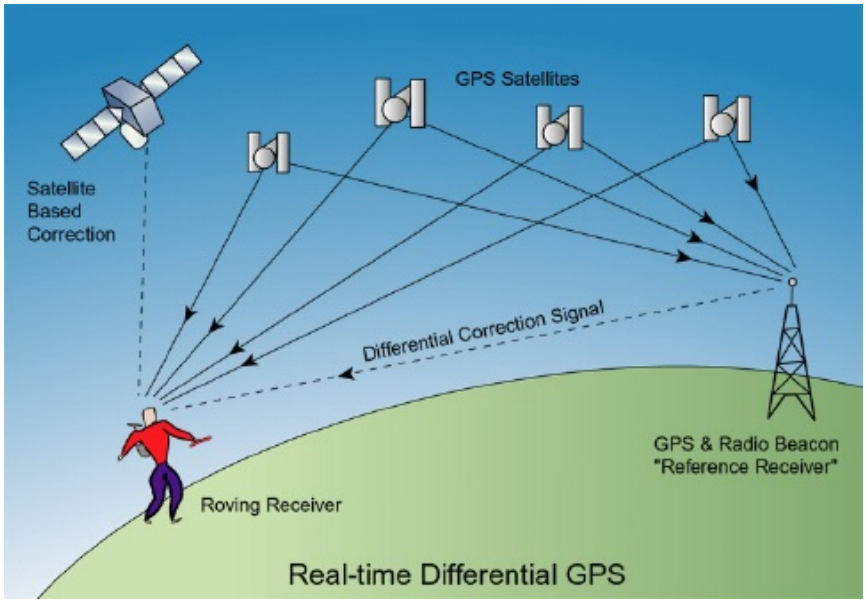

Figure 2.5: Differential GPS scheme [5]

2.5.2 Relative Positioning

The technique is known as relative positioning if we use carrier phase measurements instead of pseudorange measurements. In relative positioning, observation equations are linearized in order to minimize the common mode errors which make it different from the DGPS [26]. If the integer ambiguity is assumed to be identified, the accuracy of the position estimation, with relative positioning, becomes almost hundred times better than the DGPS technique [13].

2.6 GPS Error Sources

As we have mentioned earlier in this chapter that the GPS receiver uses trilateration technique to determine the position by measuring the distances to at least four satellites. These distance measurements are caused by several error sources. These errors may be categorized as satellite errors, propagation errors and receiver errors depending on their original resources. For high accuracy applications, these errors should be minimized as much as possible. It is not possible to eliminate these errors perfectly of course but some of these errors may be mitigated. For example, a differential processing technique is used to eliminate these errors. In this process two GPS receivers are used, one of them has known coordinates and the other one is located on the moving platform. But this process does not eliminate all the error

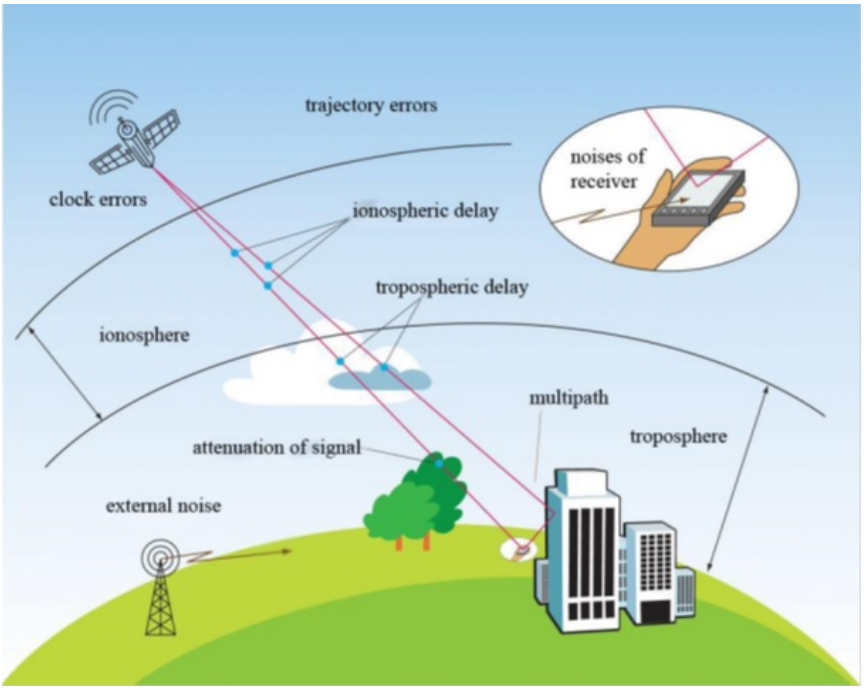

Figure 2.6: GPS error sources overview [6]

sources. Some of the common error sources are as follows

2.6.1 Satellite Orbital Errors

At the time a GPS receiver computes a satellite position, the satellite is not on the same position in the orbit. This difference is referred to as satellite orbital error or trajectory error. For real-time broadcasting, these errors are predicted by the control segment on the basis of the previous position of the satellite and the information of the Earths gravity field and then the coordinates are sent to the satellite. These errors vary from 2 to 5 meters [10].

2.6.2 Satellite Clock Error

The atomic clocks are used on the satellites which are much less affected by the gravity. But still they tend to drift a little bit from the GPS time (GPST). The control segment estimates the needed correction on the basis of the previous clock observations and then uploads these corrections to the satellite where these correction estimates are broadcasted in the navigation message [10].

2.6.3 Receiver Clock Error

The increasing development in the Integrated Circuit (IC) technology has made the GPS receivers very cheap such that a common man can easily afford it. But as a consequence, the clock accuracy is poor and biased which affects all the measurements. This biased error may be estimated by applying the kalman filtering.

2.6.4 Troposphere Delay Error

The troposphere extends from 8 to 40 km above the Earths surface. This lower part of the atmosphere is neutral which contains N_2 and O_2 and water vapors. This affects the speed of the signal by refraction. Error due to this region varies from 2.5 to 25 meter longer range depending on the elevation of the satellite. This delay in the range consists of two parts, dry one and the wet one. The 90% of the delay is caused by the dry part and the rest 10% of the delay is caused by the wet part. There are several models which can be used to minimize this error like Hopfield model, Chao model and Saastamoinen model etc [10].

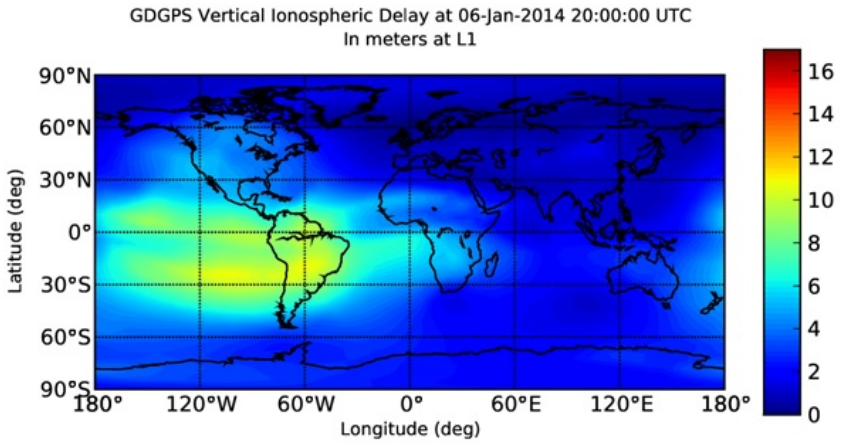

Figure 2.7: Ionosheric delay [7]

The GPS satellites are revolving around the Earth in medium Earth orbit which is approximately 20,200 KM above the surface of the Earth. A GPS satellite is transmitting signals at 50 watts or even less than this power. So a GPS receiver antenna will get relatively weak and degraded signals on the Earth due to interference [27]. The ionosphere is the upper part of the atmosphere which extends from 60 to 1000 km above the surface of the Earth. It contains a large amount of ions and free electrons. The total number of these free electrons is represented by the Total Electron Content (TEC) map as shown in the Figure 2.8 below. This TEC

is produced in real-time (RT) from the collected GPS observables by the ground stations. Mostly the signal is affected by Faraday rotation while passing through

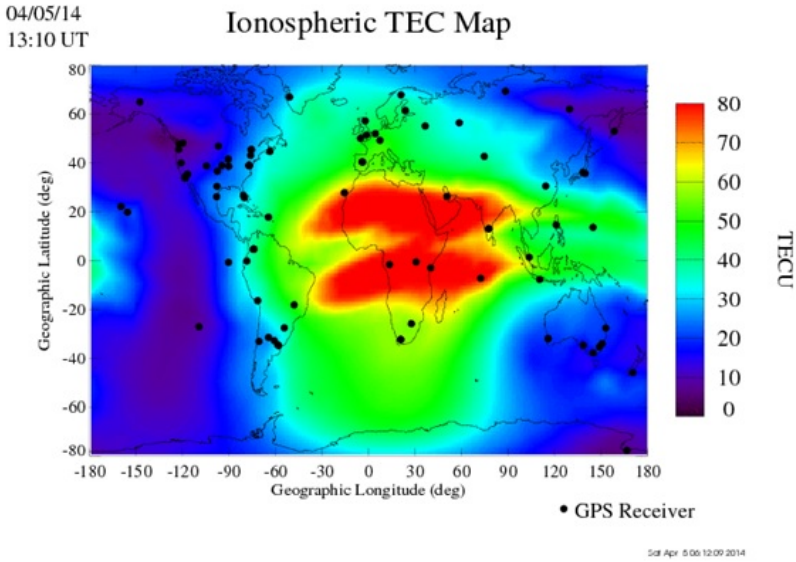

Figure 2.8: Total Electron Content Map [8]

this region. Incident wave passing through this region splits into two characteristic waves, both having different constant velocities and hence two phases. The best solution to this problem is that the receiver antenna on the GPS receiver should be circularly polarized. The probability to detect the signal will be much more but there will be a fix loss of 3 dB in the signal power [28]. Dual frequency GPS receiver may also be used to compute the accurate delay. 50 % of the delay can be reduced by using a single frequency receiver with Klobuchar model [10].

2.6.5 Multipath

The signal experiences multipath particularly in urban areas where the receiver antenna may detect the signal from other directions rather than the direct line of sight (LOS). The signals reflecting from other objects are delayed and having low signal to noise ratio (SNR). This is a major type of error source which may cause an error of 10 meters in the position.

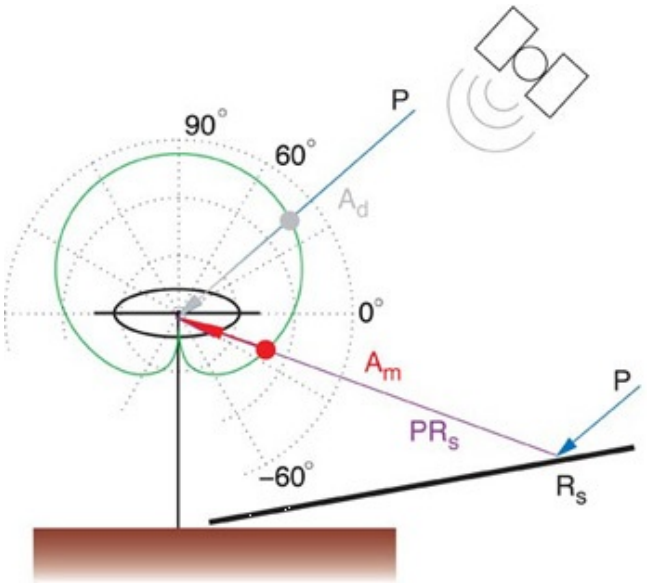

Figure 2.9: The effect of multipath [4]

2.6.6 Receiver Noise

This is the internal random noise of the receiver which is caused by different factors like the circuit elements, cables, receiver temperature and the thermal noise etc. It changes as the satellite geometry changes.

2.6.7 External Noise

External noise is concerned with the external sources. For example, interference with other signals.

2.6.8 User Equivalent Range Error (URE)

The overall error factor on the pseudo-range measurements after mitigation is called the user equivalent range error (UERE) [10].

2.7 GPS accuracy

The accuracy of a GPS receiver depends on many factors. Standalone (single receiver) GPS receiver, differential (double receiver) GPS receiver, single frequency or double frequency GPS receiver, real-time or post-processed positioning all have different accuracy levels. Even the Standard Positioning Service (SPS) provides,

minimum performance levels which means that the receiver accuracy will not be worse than a certain level for a certain period of time.

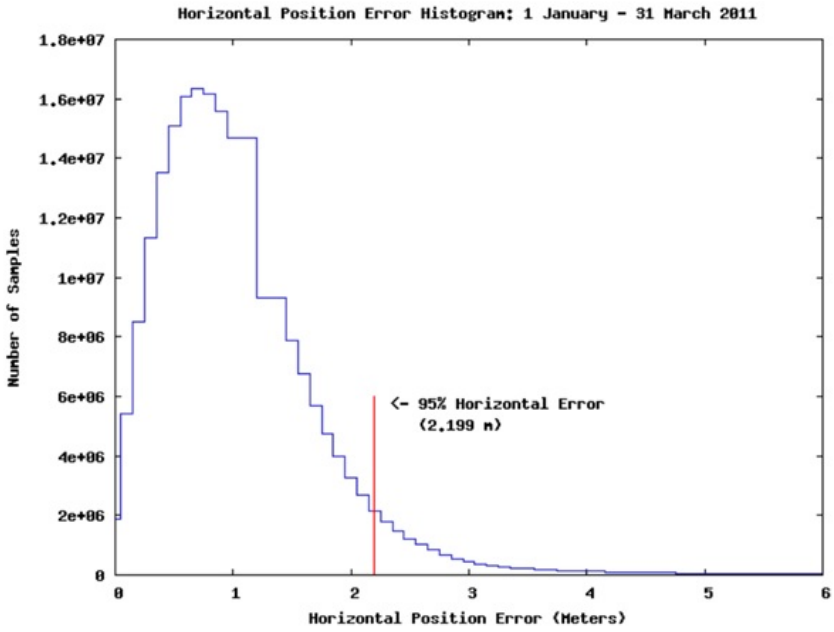

Figure 2.10: Data collected by FAA in 2011 [3]

For example, within a confidence level of 95%, pseudorange accuracy will be 7.8 meters in the worst case. Federal Aviation Administration (FAA) is collecting the real-world data as shown in the Figure 2.8 and the data show that some of the high-quality GPS receivers are capable of providing better horizontal accuracy than 3 meters and sometimes they provide even close to 1 meter. Higher accuracy can be achieved by using aided navigation systems. For example, accuracy level at few centimeters is possible by real-time positioning and a millimeter level is possible by post-mission measurements [3]. The basic level of SPS accuracy may be attained by viewing 4 satellites on a clear day and it might be difficult in urban areas. Hence the SPS accuracy varies with the position of the satellite and the time which means that the accuracy is affected by a geometric factor which is called dilution of precision or the DOP value. DOP values have different versions like geometrical dilution of precision (GDOP), positional DOP (PDOP), horizontal DOP (HDOP), vertical DOP (VDOP) and time DOP (TDOP). Smaller DOP values provide better results than the larger DOP values [29].

2.8 INS: Overview

This section provides general information about the INS structure, its basic principle along with explanation of inertial sensors.

2.8.1 Introduction

An Inertial Navigation System (INS) functions only in the inertial space which is a non-rotating frame of reference. The system depends on the Newtonian physics which is applicable only in an inertial frame. An INS is capable of measuring the position, velocity and attitude of a moving platform by the inertial sensors (accelerometers, gyros) mounted on a platform itself. It compiles the sensor measurements with the dead rocking (DR) principle which can determine the platforms current position on the basis of its previous position, sensors data and with some speed estimation of the platform. Accelerometers and gyros together form the Inertial Measurement Unit (IMU) which is then combined with the mechanization equations to form the INS [18]. The block diagram of a strapdown inertial navigation system is shown in the Figure 2.9.

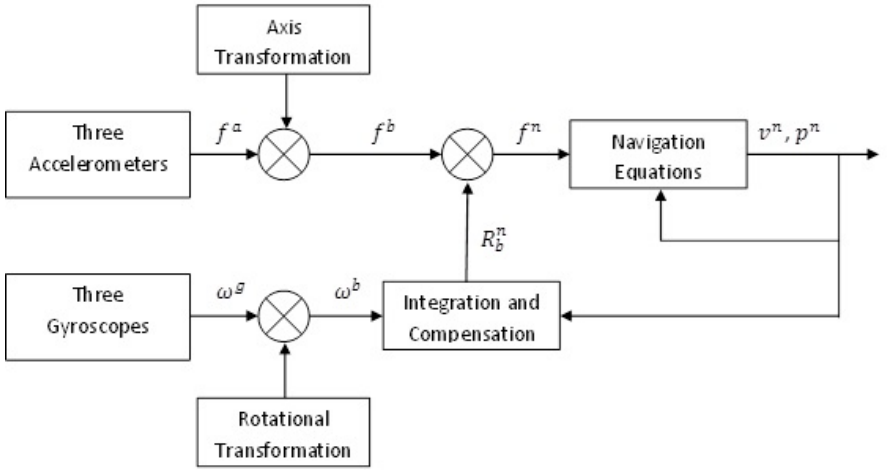

Figure 2.11: Block diagram of INS.

Since the inertial sensors measure the acceleration and rotational rates with respect to the inertial frame of reference, these measured quantities need to be transformed in several frame of references. The inertial sensors measurements are resolved along their sensitive axes (a for accelerometer and g for gyroscope in our scenario) which are usually transformed into their body frames by using

fixed-calibration matrices. Then the body to navigation frame transformations are maintain by using the body frame gyro measurements. In the end, by using a rotation matrix the body frame accelerometer measurements are transformed to the navigation frame in order to compute the position and velocity in the navigation frame [30]. An INS has different designs which have different performance characteristics, but it can be generally categorized into the following two forms.

- Gimbaled/Stable INS (SS)
- Strapdown INS (CS)
- User Segment (US)

Gimbaled/stable INS

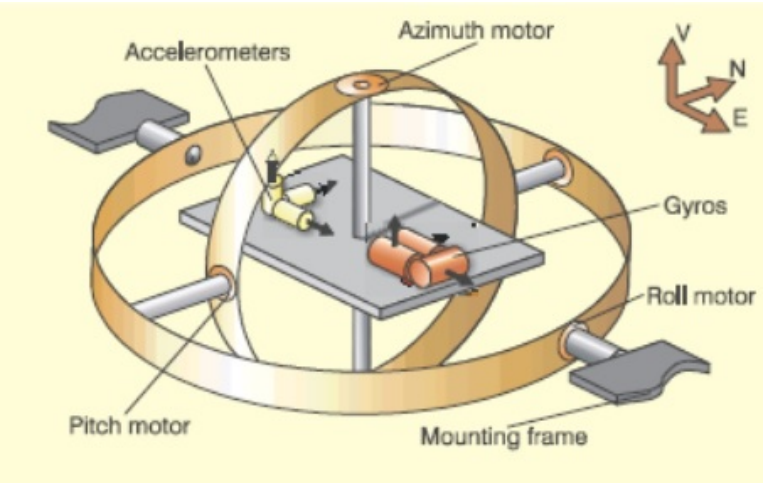

Figure 2.12: Gimbaled technology [9].

In this technology, the inertial sensors are mounted on a stable platform and they are isolated from platform rotations mechanically. The isolation is carried out by using at least three gimbals (frames) for three coordinate axes (roll, pitch, yaw). Gyroscopes are mounted on the platform which detect any rotational changes and these changes are further sent to the torque motors. The torque motors rotate the gimbals to cancel the rotational changes according to the feedback and thus the platform becomes aligned with the global frame. Ships and submarines are still using this technology.

Strapdown INS

Because of the complex mechanics involved in the platform systems (gimbaled INS), most of the modern technologies have been replaced these systems by strapdown INS. In a strapdown system, the inertial sensors are rigidly attached to the moving platform. Platform attitude is estimated by computing the rotational accelerations (vertical/horizontal) analytically by using the direction cosine matrix (DMC) which relates the body frame to the local level frame. In this study work, we will concentrate only on the strapdown systems. The strapdown systems are cheaper, smaller in size and more reliable when compared with the platform systems but computational complexity is the major drawback. The INS is dominated by the strapdown systems since the computation cost has been decreased.

The modern strapdown systems are based on the micro-machined electromechanical systems (MEMS). The performance of MEMS is improving very fast since it has become an interesting topic for the researchers and this technology offers cheap, small and lightweight inertial sensors [31]. An INS is capable of working alone but generally the output data from low-end sensors is used to update the state estimates which are determined from the integration of high-end sensor outputs and in this way the integrated or aided navigation is formed [13].

Basic Principle

An INS is based upon Newtons first law of motion which states that

A body in a state of rest or uniform motion in a straight line will continue in the same state unless some external force is applied

Since the Newtons laws of motion are applied in an inertial frame (non-rotating/non-accelerating frame), it is not easy to visualize it on the Earth. So the body must be in an inertial frame of reference.

We must not ignore the importance of Newtons second law of motion, here in the explanation of an INS, which states that

Acceleration is proportional to the resultant force and it has the same direction as that of the applied force. Mathematically

$$F = ma \tag{2.8}$$

Where,

F is the applied force, m is the body mass and a is the body acceleration due to F. An INS directly concerns to the acceleration here because by integrating the acceleration the velocity can be found and by further integration of the velocity the displacement can be determined. Hence an INS works as an integral which determines the position, velocity and attitude differences by measuring and

transforming the acceleration of a moving platform from an inertial frame to the navigation frame.

2.9 Inertial Measurement Unit (IMU)

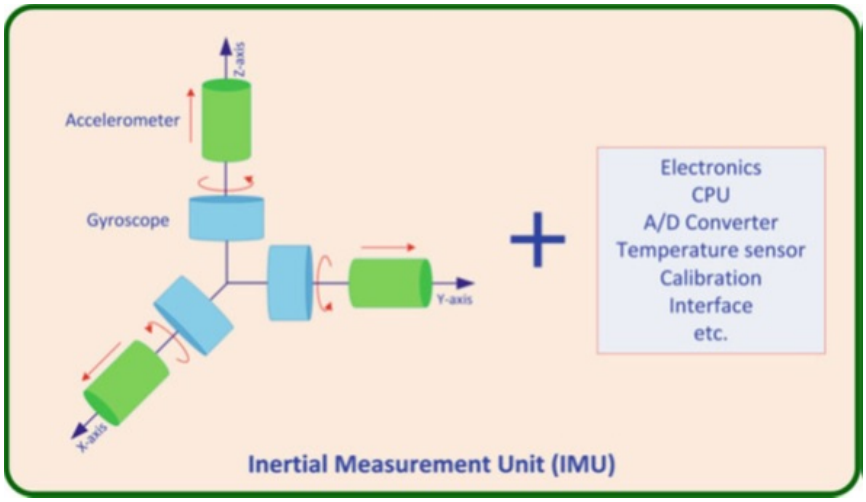

Figure 2.13: Gimbaled technology [10].

The inertial sensors (accelerometers, gyroscopes) are mounted on the platform in a common unit which is called the inertial measurement unit (IMU). Three accelerometers are mounted orthogonally to three gyroscopes. The linear motion of the platform along with the three mutually perpendicular directions is measured by the accelerometers while the rotational motion in the same directions is measured by the gyroscopes. Both types of sensors have the same origin and axes which are fixed on the platform and that is why this is called the body frame. Despite the inertial sensors, an IMU also contains electronics to perform the calibration operations and computation of other algorithms [10].

2.9.1 Inertial sensors

Inertial sensor observations are relative to the inertial space which is a perfect space (mass center of the universe). Please note that mechanical gyroscopes and accelerometers are introduced here in order to understand the basic principle of the IMU. There are two most common types of inertial sensors which are normally used in an IMU.

- Accelerometer

- Gyroscope

Accelerometers

An INS depends on the acceleration measurements which could be integrated further to compute the changes in velocity and position. The acceleration is measured internally while the velocity and position requires an external reference. An

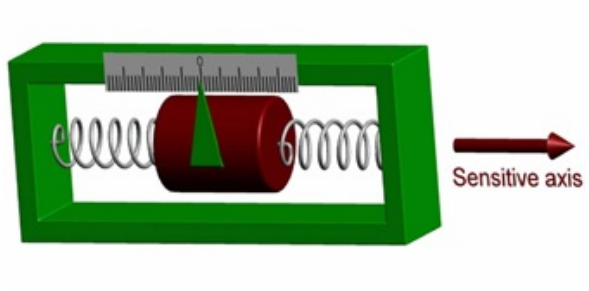

Figure 2.14: Physics of an accelerometer [11].

accelerometer is used to sense the acceleration (linear motion in three mutually perpendicular directions). Accelerometers are rigidly attached to the platform in a strapdown INS. The two typical design techniques are open loop and closed constructions [15] [10, ch 6]. An open loop accelerometer is basically a proof mass attached to a pair of springs from both sides and the other sides of these springs are attached to a case. This attachment is adjusted horizontally to align it along the sensitive axis of the accelerometer. When the platform starts accelerating, it displaces the mass from its initial position (equilibrium state). Hence the displacement is detected along that particular axis. But in the case when the sensitive axis of the accelerometer is aligned vertically under the influence of a gravitational field, the attached mass will move downwards showing positive acceleration. The displacement and the acceleration both are in the same direction in this case which creates a confusion in the mind. The principle of equivalence clears the confusion by explaining the fact that the measurement taken by an accelerometer at some point in a terrestrial frame, inertia and navigation can not be separated. The accelerometer output is a negative of the acceleration in inertial space [10]. This output is because of the gravitational field and is called the specific force which is written as

$$F = a - g \tag{2.9}$$

where,

f = Specific force

g= Acceleration due to gravity

a= Acceleration in space (kinematic acceleration).

The equation 2.9 is called the navigation equation because by integrating the acceleration, navigation quantities such as velocity and position can be found. The closed loop technique is used for more accurate instrument design. In this technique the displacement is calibrated to zero position because the position measurements are more accurate than the displacement measurements. In this design, the springs are replaced by an electromagnetic device (pair of coils) which tries to maintain the zero position of the proof mass by exerting a force on the proof mass. Any deflection causes a potential which force the proof mass to its zero calibration [15] [10]. A good commercial accelerometer may have an accuracy of 50 μg.

Gyroscopes

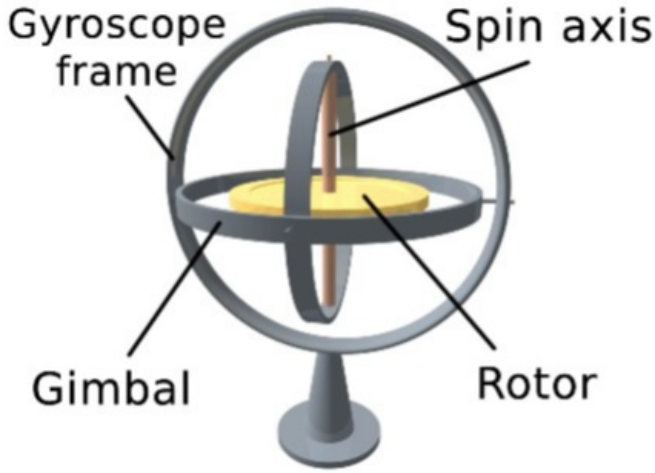

Figure 2.15: Gyroscope with its spin axis and rotor [12].

The motion of a body in three dimensions involves the rotational and translational motion. Gyroscopes are used to measure these angular rates with respect to an inertial frame of reference. The integration of these angular rates provides the change in the angle with respect to an initial reference. Hence it measures the attitude of a platform or the angular rate depending on the type of gyroscope used. There are many types of Gyroscopes like mechanical or optical gyroscopes etc. The most basic form of the gyroscope is the mechanical or conventional gyroscope which is mostly used in strapdown navigation applications [15]. A mechanical gyroscope basically maintains the angular momentum by utilizing the inertial properties of a high speed wheel. Any change in the angular momentum with

respect to the inertial frame of reference is resisted by the spinning wheel. The wheel is isolated from the platform by using gimbals and any change in the gimbal position is recorded as an output of the gyroscope. The wheel continues its spin along the direction of its spin axis in the influence of its angular momentum which can be determined by multiplying the speed of the wheel by the inertia as shown below [15] [10].

$$H = I\omega_s \tag{2.10}$$

Where,

H denotes the angular momentum, I denotes the inertial momentum and ω_s denotes the angular velocity.

Ring Laser Gyroscope (RLG)

The Ring Laser Gyros (RLG) are used for precise rotational measurements. These gyros are critical sensors used for navigation in air and sea, vehicle stabilization, targeting and attitude and heading reference systems (AHRS). An RLG is based on the sagnac effect as shown in the figure below. According to this phenomena, the

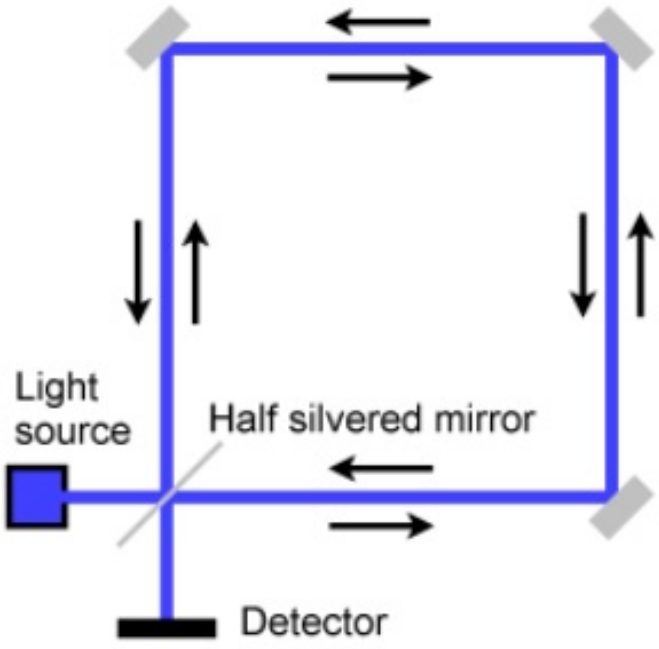

Figure 2.16: Sagnac effect [4].

inertial property of the light is exploited by emitting two counter-propagating laser

beams in a loop. The beam propagating clockwise will travel a longer distance than the anti-clockwise propagating beam if the loop is rotating clockwise, leading different frequencies (interface) and this difference is depending on the rotation rate. By measuring the difference, the rotation rate along the sensitive axis of the gyro can be determined. Hence the orientation of a system can be found in an inertial frame [4].

2.10 MEMS Based Inertial Sensor Technology

Heavy and costly IMU have been used in navigation systems for a long time. These traditional sensors are now replaced by the new technology of Micro Electrical Mechanical Sensors (MEMS). This technology has successfully solved some of the main problems of the inertial sensors like size, price and weight and that is why they are frequently used in many GPS/INS integrated systems [32]. The combination of a GPS/INS integrated system and low cost MEMS sensors create a great tracking attraction for a Land Vehicle Navigation system (LVNS). It offers accuracy, reliability and continuity while GPS outages [2]. Finally, the system performance is better than any of the standalone systems.

2.10.1 Low-Cost MEMS-Based Inertial Sensors

In the growing market of navigation systems, the device cost plays an important role. The competition for providing a low cost GPS/INS integrated system has played an important role in developing the MEMS inertial sensors technology. This technology takes the advantage of massive production and easy packaging. Small, robust and low cost inertial sensors are available in the markets for navigation applications which were not easily possible in the past because of the big size and heavy cost [2]. For commercial applications like LVNS, MEMS is the cheapest technology available in the market today [33]. Particularly accelerometers and gyroscopes have been mainly focused in the field of MEMS research due to the rapidly increasing market of the navigation system devices like vehicle GPS receivers [34]. MEMS accelerometers have been developed earlier and then the MEMS gyroscopes were developed [2].

MEMS-Based Accelerometers

A MEMS accelerometer measures the acceleration on the basis of capacitive sensing. It is made up of a proof mass lies in the center of two silicon electrodes. Any disturbance of the proof mass will cause a change in the capacitance. This amount of change will then measure the disturbing force. This terminology is

known as open loop method [2]. There is another terminology which is known as closed loop. According to this terminology, acceleration is measured by measuring a counteracting force which keeps the proof mass at zero-deflection point [34]. These MEMS based accelerometers are used in many applications like automotive air bags and modern vehicle industries [2].

MEMS-Based Gyroscopes

MEMS based gyroscopes are newly developed technology relative to the MEMS based accelerometers. Most of the MEMS based gyroscopes simply measure the angular rates. They do not measure the absolute angles [34]. A MEMS gyroscope is basically a vibrating sensor oscillating with constant amplitudes. If the system is moved out of its internal vibration plane, the Coriolis Effect forces the sensor to oscillate out of the plane [2]. The capacitors are used as sensors which observe oscillations out of the plane to measure the angular rates.

2.10.2 MEMS Performance and Error Sources

Despite of the great development in MEMS technology, stand-alone navigation systems can compensate a small amount of error for a very short period of time during GPS outages. This happens because the sensor errors grow very fast. Despite of the fact that static and kinematic models show improved performance of MEMS based inertial sensors by implementing autoagressive models but still the test results are not good enough during long term GPS outages [35]. MEMS sensor errors are normally estimated before their use. Typical low cost MEMS sensor errors are bias and scale factor [32]. The exact information about the sensor behavior is the key factor in order to predict its performance and design analysis. On the other hand, stochastic type of error sources like rate ramp, quantization noise, rate random walk, and bias instability also exist in inertial sensors. These errors are analyzed by applying autoagressive (AR), Gauss-Markov (GM), Power Spectral Density (PSD) and Allan Variance (AV) methods [36]. Since the MEMS technology is continuously improving so one should carefully select the latest MEMS sensors available in the market. A kalman filter can be implemented in order to enhance the performance of navigation parameters.

Chapter 3

Reference Frames and Transformation

Earth is not a stone and the mass of the Earth is moving all the time. There are differences in the layers of the Earths crust and the tectonic movements need to be analyzed. So the reference frames are moving with different velocities with respect to each other and therefore they need to be reproduced all the time and they should be four dimensional. Despite of the three dimensional orthogonal coordinates the fourth dimension should be included which is the time. Different sensors provide the information with respect to a particular frame of reference and the coordinates of that frame of reference are typically different from the navigation frame. For example, the position of an antenna is estimated in the Earth Centered Earth Fixed coordinates by the GPS which needs to be transformed to the navigation frame to make it consistent with the other sensor measurements [13].

3.1 Properties

Navigation quantities are measured in different reference frames. Properties of these frames must be clarified in order to insure the communications and interoperations among the multi discipline engineering environments [13].

- A notation must be required to represent the reference frame.
- Boldface letters are used to represent the vectors and matrices.
- A particular reference frame relative to a vector is represented b y a superscript. For example, The rotation matrix transforming a vector from frame a to b is written as

$$\alpha^b = C_a^b \alpha^a \tag{3.1}$$

Where $alpha$ represents the vector, C is the rotation matrix, subscript and superscript are representing the initial and the transformed frames of reference respectively.

- All the three axes of a reference frame are supposed to be mutually perpendicular to each other and also following the right handed rule.
- Geoid is the mean sea level and the gravity vector is normal to the geoid overall. It is convenient to consider an ellipsoidal model to approximate the geoid.
- Geodetic or geocentric ellipsoidal coordinates may be used but the local geographic frame must align with the normal of geodetic or geocentric coordinates.
- Origin of a reference frame may be defined by the following two methods.

    1. The projection of a point P on the reference ellipsoid. In this scenario, the origin moves as the point P moves as shown in the Figure 3.1.

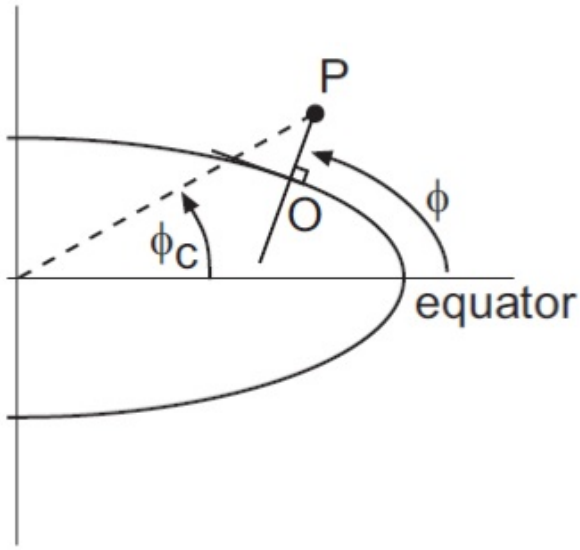

Figure 3.1: Difference between geodetic and geocentric latitude [13]

2. In the second method the origin is fixed at a suitable point for local frame of reference. In this scenario, the origin of the local frame does not move with the movement of the point P as shown in the Figure 3.2. There are several frames of reference which are frequently used

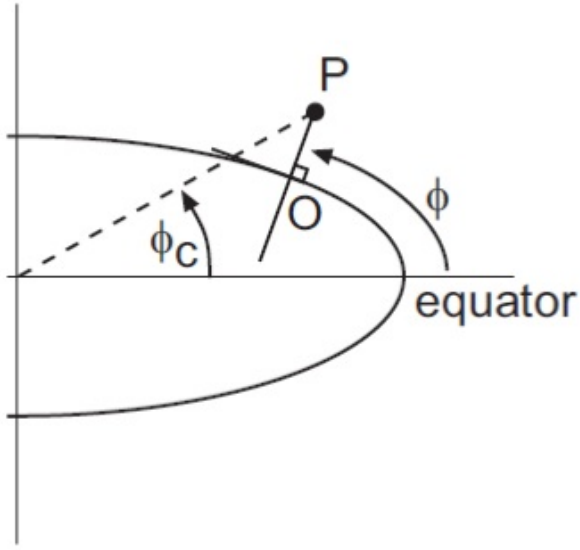

Figure 3.2: Local frame of reference [13]

in most of the navigation applications but just some of them have been used in this study work and they are briefly described in the following section.

3.2 Inertial Frame (i-frame)

Inertia is the property of a body to maintain its uniform velocity unless some external force or torque is applied on it (Newtons first law of motion). An inertial frame of reference is the one in which Newtons laws of motion are applicable. This frame of reference is non-rotating and non-accelerating with respect to the stars and galaxies [18]. Coordinate axis are mutually perpendicular to each other in any direction with an arbitrary origin. Sometimes an Earth Centered Inertial (ECI) frame is defined with its origin coincident with the center of mass of the Earth at some particular incident of time. The z-axis of this frame is taken as parallel to the Earths instantaneous spin axis, x-axis points towards the mean vernal equinox (a

fixed direction in space) and the y-axis completes a right handed orthogonal coordinate system. The ascending node between the elliptic and the celestial equator represents the vernal equinox [14].

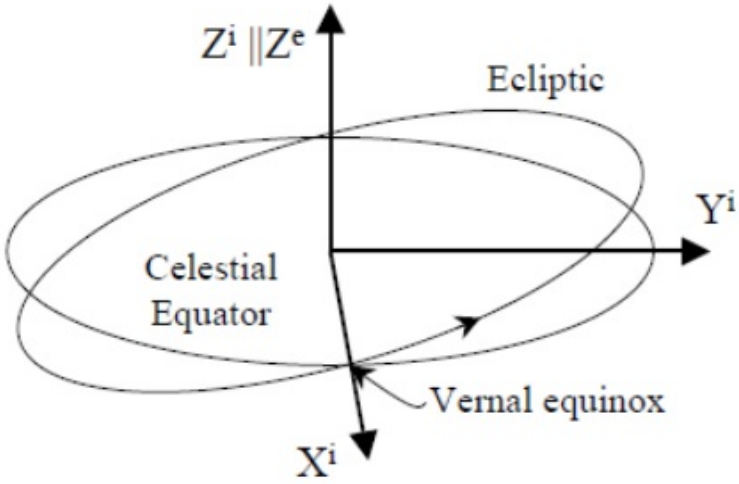

Figure 3.3: Inertial frame of reference [14]

3.3 Earth Centered Earth fixed Frame (e-frame)

The origin of the Earth Centered Earth Fixed frame of reference is fixed to the mass center of the Earth. The x-axis intersects the prime meridian and the equatorial plane, z-axis is parallel to the mean spin axis of the Earth and the y-axis is mutually perpendicular to both x-axis and z-axis which forms a right-handed orthogonal coordinate system.

Since the origin of the e-frame is fixed to the Earth, the axes of e-frame rotate with respect to the inertial space with a frequency

$$\omega_{ie} \approx 7.292115 \times 10^{-5}(rad/sec) \tag{3.2}$$

This means ECEF frame is not an inertial frame of reference [13]. There are two types of ECEF frames rectangular and geodetic reference frames. We will concentrate on the latter one in this study work [30].

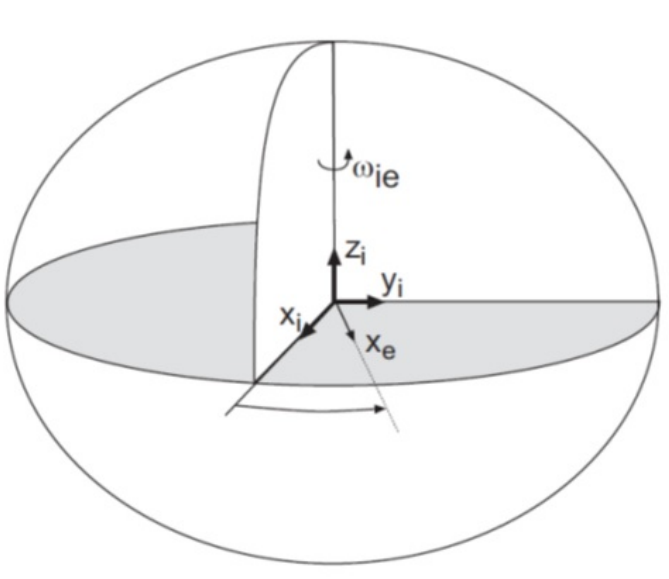

Figure 3.4: Rotation of ECEF frame with respect to ECI frame [13]

3.4 Body or Vehicle Frame (b-frame)

The position and velocity of a vehicle is computed by inertial sensors mounted in an IMU which is rigidly attached to the vehicle of interest. In strap-down navigation systems the IMU is usually aligned with frame of vehicle and the center of gravity of the IMU is assumed to be the origin which helps to simplify the derivations of the kinematic equations [30]. The forward direction of the vehicle is taken as x-axis, downward direction is represented by z-axis and y-axis is mutually perpendicular to both of these axes and it forms a right-handed coordinate system. The rotation around x-axis is represented by roll (φ), the rotation around y-axis is represented by pitch (θ) and the rotation around z-axis is represented by yaw (ψ) [4].

3.5 Body to navigation frame rotational transformation

The alignment of body frame and navigation frame is carried out by applying a number of rotations about the coordinate axes [33]. These angular rotations about x, y and z-axis are known as Euler angles and are called roll (φ), pitch (θ) and yaw (ψ) respectively. Hence a series of three rotations will form the direction cosine matrix (DCM). The DCM transforming b-frame to navigation frame can be

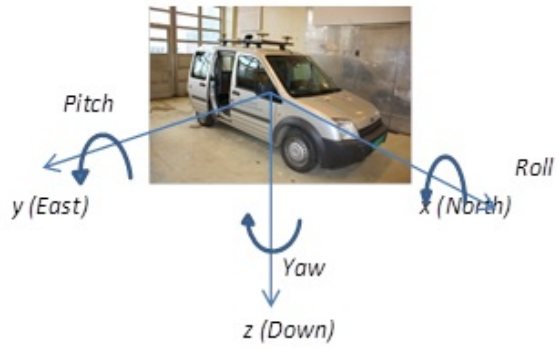

Figure 3.5: Euler angles representation in vehicles frame.

expressed in the following way [14].

$$C_b^n = (C_n^b)^T = R_z(-\psi)R_y(-\theta)R_x(-\phi) \tag{3.3}$$

$$C_b^n = \begin{bmatrix} cos(\psi) & -sin(\psi) & 0 \\ sin(\psi) & cos(\psi) & 0 \\ 0 & 0 & 1 \end{bmatrix} \begin{bmatrix} cos(\theta) & 0 & sin(\theta) \\ 0 & 1 & 0 \\ -sin(\theta) & 0 & cos(\theta) \end{bmatrix} \begin{bmatrix} 1 & 0 & 0 \\ 0 & cos(\varphi) & -sin(\varphi) \\ 0 & sin(\varphi) & cos(\varphi) \end{bmatrix} \tag{3.4}$$

$$C_b^n = \begin{bmatrix} cos(\psi)cos(\theta) & -sin(\psi)cos(\varphi) + cos(\psi)sin(\theta)sin(\varphi) & sin(\psi)sin(\varphi) + cos(\psi)sin(\theta \\ sin(\psi)cos(\theta) & cos(\psi)cos(\varphi) + sin(\psi)sin(\theta)sin(\varphi) & -cos(\psi)sin(\varphi) + sin(\psi)sin(\\ -sin(\theta) & cos(\theta)sin(\varphi) & cos(\theta)cos(\varphi) \end{bmatrix} \tag{3.5}$$

3.6 Instrument frame

An instrument frame of reference is marked on the case of the instrument itself. Sensor measurements are resolved then with respect to the sensitive axes of the instrument. In real world the sensitive axes of the instrument is not aligned with the reference frame of the instrument due to imperfections. But improvements are possible by compensating the scale factor and taking care of the temperature and linearity parameters. Precise calibration and orthogonalization routines can make a difference. These calibrations are done in the factory or during the instrument operation [13].

3.7 Geographic Frame or the Navigation Frame (g-frame, n-frame)

Its a local reference frame with respect to the geoid of the Earth (average sea level) and is also called geographic frame (g-frame) or navigation frame (n-frame). The x-axis points toward the geodetic north, z-axis points toward the interior of the Earth and y-axis points toward the east to form the right-handed coordinate system, i.e. north east down (NED) frame of reference. The geographic frame is not an inertial frame of reference because the origin of the frame travels with the vehicle and the coordinates of the frame rotate relative to the inertial space. The advantage of an east north up (ENU) coordinate system is that the altitude increases in the upward direction but in case of an NED coordinate system the advantage is the positive direction relative to the downward direction while a vehicle is turning to the right. The other advantage is that the system coordinates coincide with the fixed coordinates of the vehicle while it is heading to north with a leveled position. Since the use of these systems is very common and practical, a lot of research work can be found on these systems [14].

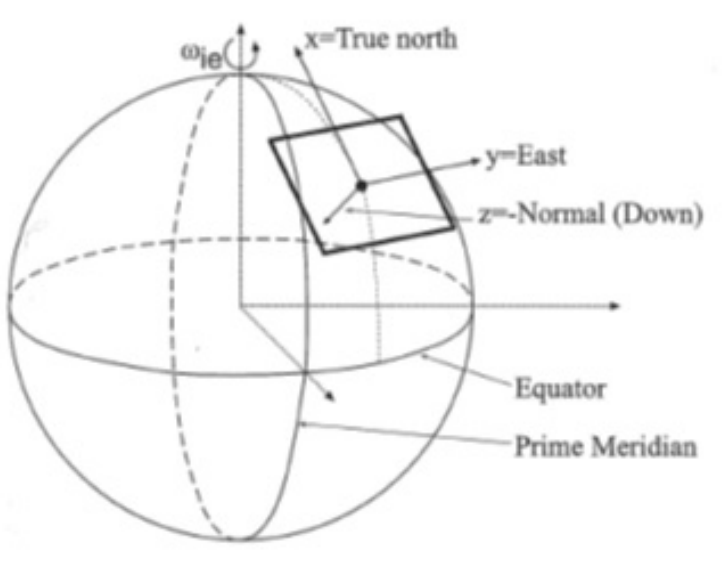

Figure 3.6: Local geographic plane relative to ECEF frame [13]

3.8 Earth to navigation frame rotational transformation

GPS measurements are in e-frame usually. Navigation measurements are transformed into e-frame by the rotation of coordinate systems about y-axix and z-axis. The transformation from e-frame to n-frame can be expressed by the following direction cosine matrix (DCM) [14].

$$C_e^n = R_y(-\varphi - \frac{\pi}{2})R_y\lambda \tag{3.6}$$

$$C_e^n = \begin{bmatrix} -sin(\varphi)cos(\lambda) & -sin(\phi)sin(\lambda) & cos(\phi) \\ -sin(\lambda) & cos(\lambda) & 0 \\ -cos(\varphi)cos(\lambda) & -cos(\varphi)sin(\lambda) & -sin(\varphi) \end{bmatrix} \tag{3.7}$$

Where φ and λ represent the latitude and the longitude respectively. Ry and Rz represent the rotational matrices about y-axix and z-axis respectively. By exploiting the orthogonality property, the transformation from n-frame to e-frame can be expressed by the following direction cosine matrix [14].

$$C_n^e = (C_e^n)^{-1} = (C_e^n)^T \tag{3.8}$$

$$C_n^e = \begin{bmatrix} -sin(\varphi)cos(\lambda) & -sin(\lambda) & -cos(\varphi)cos(\lambda) \\ -sin(\varphi)sin(\lambda) & cos(\lambda) & -cos(\varphi)sin(\lambda) \\ cos(\varphi) & 0 & -sin(\varphi) \end{bmatrix} \tag{3.9}$$

Chapter 4

INS System Kinematics

In classical mechanics, the study of motion of points, objects or groups of objects, ignoring the causes which create that motion, is known as kinematics. In other words the geometry of the motion is explained by kinematics. It explains the trajectories of points and their differential properties such as displacement, velocity and acceleration [1]. Accelerometers and gyros, rigidly attached to the platform of the vehicle of interest in a strapdown INS, are used to measure these quantities. Gyros bias and scale factor is very important because at each maneuver of the vehicle, rotational rates are sensed by the gyros. On the other hand, accelerometers sense the specific force [13].

There are three types of kinematic equations involved in an INS .

- Position
- Velocity
- Attitude

The navigation equation which represents the angular rotations between any two coordinate systems is written as [30].

$$\frac{\mathrm{d}^2\rho^b}{\mathrm{d}t^2} = \frac{\mathrm{d}^2\mathbf{R^b}}{\mathrm{d}t^2} + \mathbf{R}_a^b\left[2\Omega_{ba}^a\mathbf{v}^a + \Omega_{ba}^a\Omega_{ba}^a\mathbf{r}^a + \dot{\Omega}_{ba}^a\mathbf{r}^a + \frac{\mathrm{d}^2\mathbf{r^a}}{\mathrm{d}t^2}\right] \tag{4.1}$$

Where a, b are representing any two coordinate systems, R is the vector between the origins of the both frames, r is the vector from origin of a-frame to the point P, and denotes the vector from origin of b-frame to the point P. Many navigation systems are based on this equation. Navigation Transformation between

different frames of reference is possible by differentiating these equations. Reference frame rotational transformations are maintain by using the method of direction cosines in this study work. Particular selections for a-frame will be analysed and differential equations for these frames will be given in the following section. Detailed derivation of equations can be found in [30].

4.0.1 Navigation frame kinematics

Navigation or local geographic frame mechanization is commonly used to measure the navigation quantities for long distance navigation applications around the Earth. Although Earth frame or inertial frame can be used to compute theses quantities but the vector transformations involved more complexity. In this study work we will choose the navigation frame to compute the navigation quantities in order to avoid these complexities.

4.1 Gyro observations

Gyroscopes measure the turn rate or changes in the attitude of a vehicle relative to the inertial frame of reference and these changes are actually in the direction of the cosine matrix. The observation equation for the gyroscope can be written as

$$\omega_{nb}^{b} = \omega_{ib}^{b} - C_{n}^{b}[\omega_{ie}^{n} + \omega_{en}^{n}] \tag{4.2}$$

$$\omega_{nb}^{b} = \omega_{ib}^{b} - C_{n}^{b}\omega_{ie}^{n} - C_{n}^{b}\omega_{en}^{n} \tag{4.3}$$

4.2 Accelerometer observations

As mentioned earlier in the chapter 2, the accelerometers measure the difference between the vehicle acceleration in space (also called the true acceleration) and the acceleration due to the force of gravity and this difference was called as the specific force. The observation equation model for the accelerometer in the navigation frame can be written be as [15][10].

$$\dot{v}^{n} = C_{b}^{n} f^{b} - (2\omega_{ie}^{n} + \omega_{en}^{n}) \times v_{e}^{n} + g_{l}^{n} \tag{4.4}$$

The accelerometer measures the specific force in the body frame, we need to resolve its components into the navigation frame since we have chosen the navigation frame.

$$\dot{v}^{n} = f^{b} - (2\omega_{ie}^{n} + \omega_{en}^{n}) \times v_{e}^{n} + g_{l}^{n} \tag{4.5}$$

The model terms are briefly explained below. For detail derivation of the model see chapter 3 in [15] [10].

f^n is the specific force measured by a group of three mutually perpendicular single axis accelerometers and the components of the specific force are resolved in the navigation frame.
v_e^n is the velocity relative to the e-frame and expressed in the navigation frame.
ω_{ie}^n is the Earths rotational rate resolved in the navigation frame.
ω_{en}^n is the rotational rate of the navigation frame relative to the e-frame.
g_l^n is the gravity vector which is equal to the gravitational vector less the centripetal acceleration due to the Earths rotation in the i-frame.
Then the turn rates of the body can be computed as

$$\hat{C}_b^e = C_b^e + \dot{C}_b^e \Delta t \tag{4.6}$$

where,

$$\dot{C}_b^e = C_b^e . \Omega_{eb}^b$$

The Earth rotation rate as given in [13] is

$$\omega_{ie} \approx 7.292115 \times 10^{-5} \text{rad/sec}$$

Thus the Earth rotational rate vector relative to the inertial frame and projected in the e-frame can be expressed in the following way

$$\omega_{ie}^e = (0 \quad 0 \quad \omega_e)^T$$

Where, ω_e represents the magnitude of the Earths rotational rate. This rotational rate can be projected from e-frame to the navigation frame by using the DCM C_e^n [14].

$$\begin{aligned} \omega_{ie}^n &= C_e^n \omega_{ie}^n \\ \omega_{ie}^e &= (\omega_e cos\varphi \quad 0 \quad -\omega_e sin\varphi)^T \end{aligned} \tag{4.7}$$

The equation (4.7) is also called the transport rate which may be expressed in terms of time derivatives of the longitude and latitude [15][10].

$$\omega_{en}^n = (\dot{\lambda} cos\varphi \quad -\dot{\varphi} \quad \dot{\lambda} sin\varphi)^T \tag{4.8}$$

The time derivatives of the longitude and latitude are defined as

$$\dot{\varphi} = \frac{v_N}{(M+h)}$$
$$\dot{\lambda} = \frac{v_E}{(N+h)}$$

Thus,

$$\omega_{en}^n = \begin{bmatrix} \frac{v_E}{(N+h)} \\ -\frac{v_N}{(M+h)} \\ -\frac{v_E tan\varphi}{(N+h)} \end{bmatrix}$$

Where v_N, v_E represent the north and east velocities, respectively.

4.3 Local gravity vector

The local gravity vector is a combination of both accelerations, due to mass attraction force and centripetal force. Thus gravitational field vector and gravity field vector are different [15] [10 p.27]. Because of the rotation of the Earth, usually gravity field vector is used and is written as

$$\begin{aligned} g &= \bar{g} - \omega_{ie} \times [\omega_{ie} \times r] \\ g &= \bar{g} - \Omega_{ie}\Omega_{ie} r \end{aligned} \tag{4.9}$$

The north and east components are zero since the normal gravity vector coincides

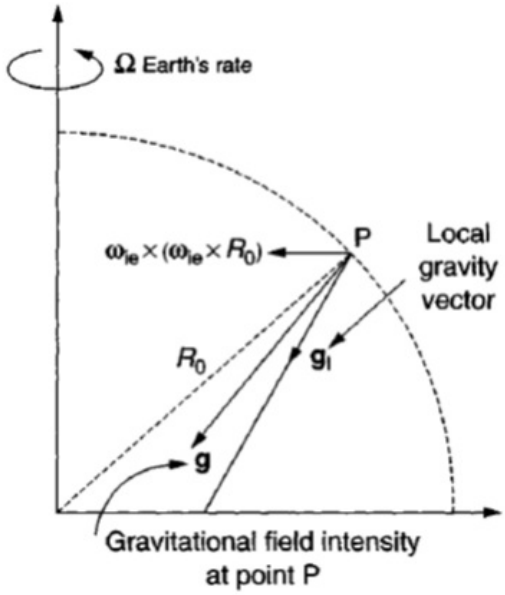

Figure 4.1: Gravitational field components

with the ellipsoidal normal on the ellipsoid [10]. The local gravity vector in NED frame can be written as

$$\begin{aligned} g^l &= [0 \quad 0 \quad -g]^T \\ g^l &= [0 \quad 0 \quad -9.80665]^T \end{aligned} \tag{4.10}$$

4.4 Detailed Inertial Navigation Equations

The motion of a vehicle can be described mathematically by the equation of motion which described the first order time derivatives of a system. The state variables position, velocity and rotation matrix can be expressed by a three dimensional state vector in the following way [26].

$$\dot{x}^a = (\dot{r}^a \quad \dot{v}^a \quad \dot{R}_b^a)^T \tag{4.11}$$

Where a represents the relative frame of the state vector, dot represents the time derivative and r,v,R represent position vector, velocity vector and rotation matrix respectively. All the three time derivatives, position, velocity, and rotation matrix needs to be analysed in order to transform the equation of motion in the navigation frame. Thus the position of a body in navigation frame can be written by using the curvilinear coordinates [14].

$$\dot{r}^n = (\varphi \quad \lambda \quad h)^T \tag{4.12}$$

The velocities in the navigation frame are given as [14]

$$v^n = \begin{pmatrix} v_N \\ v_E \\ v_D \end{pmatrix} = \begin{pmatrix} (M+h) & 0 & 0 \\ 0 & (N+h)cos\varphi & 0 \\ 0 & 0 & -1 \end{pmatrix} \begin{pmatrix} \dot{\varphi} \\ \dot{\lambda} \\ \dot{h} \end{pmatrix}$$

The rearrangement of the above equation gives the time derivatives of the coordinates.

$$\dot{r}^n = \begin{pmatrix} \dot{\varphi} \\ \dot{\lambda} \\ \dot{h} \end{pmatrix} = \begin{pmatrix} \frac{1}{(M+h)} & 0 & 0 \\ 0 & \frac{1}{(N+h)cos\varphi} & 0 \\ 0 & 0 & -1 \end{pmatrix} \begin{pmatrix} v_N \\ v_E \\ v_D \end{pmatrix}$$

Where M and N are the radii of the curvature and h is the ellipsoidal height. Radii of curvature are expressed as

$$N = \frac{a}{(1 - e^2 sin^2\varphi)} \tag{4.13}$$

$$M = \frac{a(1-e^2)}{(1 - e^2 sin^2\varphi)^{3/2}} \tag{4.14}$$

Where a and e represents the semi-major axis and linear eccentricity of the ellipsoid.

4.5 Rotation and transformation of a vector

Rotation and transformation are two different terminologies while representing the attitude of a vehicle. Mixing these definitions may results wrong calculations or unexpected attitude of the vehicle [29]. The operation of rotation actually modifies the representation of the rotating vector in a coordinate system say X. If the coordinate system X and the vector are represented in another coordinate system say Z, then a rotation will change the orientation of the vector in both coordinate frames X and Z. The transformation, on the other hand, is the representation of the vector relative to another coordinate system say Y. But the representation of the vector and X, Y coordinate systems in a third coordinate system Z, will not change the orientation of the vector in Z.

4.6 Attitude representation

Rotations about different axes change the attitude of a vehicle. Note that the attitude change is not just depending on the small deflections in the rotational angles about axes but also on the sequence in which these changes are happening [15][10]. Axis of rotations are defined in the figure below. Attitude of a vehicle with respect

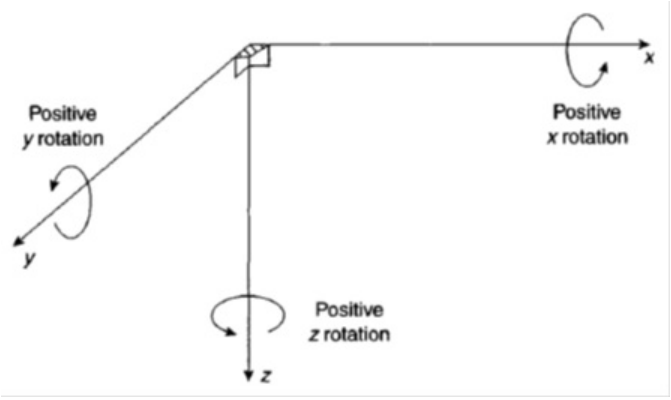

Figure 4.2: Orthogonalright-handed axes of rotations [15].

to a specific reference frame can be represent by several mathematical descriptions. But three of them are commonly used.

- Direction cosines
- Euler angles
- Quaternions

4.6.1 Direction cosines

The direction cosine matrix (DCM) also known as rotation matrix, is a 33 orthogonal matrix. Unit vectors in the body axes are projected along the reference axes by using DCM. A body to navigation frame DCM can be written in its component form.

$$C_b^n = \begin{pmatrix} C_{11} & C_{12} & C_{13} \\ C_{21} & C_{22} & C_{23} \\ C_{31} & C_{32} & C_{33} \end{pmatrix} \tag{4.15}$$

A DCM can transforms the coordinates of a vector from one frame of reference to another frame of reference. For example, when vector in an orbitrary frame b is multiplied by a DCM C_b^n (body to navigation frame DCM), then the resultant vector will have coordinates in the navigation frame [15] [10].

$$r^n = V_b^n r^b \tag{4.16}$$

From equation (4.16), The Euler angles can be found in the following way.

$$\theta = -\tan^{-1}\left(\frac{C_{31}}{\sqrt{1 - C_{31}^2}}\right) \tag{4.17}$$

$$\phi = atan2(C_{32}, C_{33}) \tag{4.18}$$

$$\psi = atan2(C_{21}, C_{11}) \tag{4.19}$$

Where atan2 is a 4-quadrant inverse function of tangent. Since we are using direction cosine matrices through out this study work, so the rest of the two representations are just briefly defined below.

4.6.2 Euler angles

This is a simple method which may be used for transformation between frames of reference. Three successive rotations about different axes are involved in this method.

4.6.3 Quaternions

This method is based on Eulars rotational theorem and is also a widely used representation. In this method only one rotation about a predefined vector in the reference frame is required for transformation between any two reference frames [37].

Chapter 5

GPS/IMU Integration

The integrated GPS/IMU solution provides more robust and reliable system than either of the standalone system, especially in the urban environments where the GPS only approach is not adequate [20]. Both of the systems are complementary to each other. Most important complementary characteristics of these systems are listed in the Table 5.1.

GPS	INS
Pseudorange	Angular velocity and acceleration
Good long time absolute accuracy	Good short time relative accuracy
Geometry dependent Clear sky view is required for good accuracy	Initial attitude dependent Self contained
Low data rate (1-10 Hz)	High data rate (50-500 Hz)

Table 5.1: Characteristics of GPS/INS

There are a number of approaches used for GPS/INS integration which may be adopted and many of them have been investigated for different grades of IMUs. There are three most common integration strategies used for GPS/INS integration today [18] as listed below.

- Loosely Coupled Integration
- Tightly Coupled Integration
- Ultra-tight Integration

Since ultra-tight integration is implemented only by the hardware manufacturers therefore we will focus just on the two broad classes of GPS/INS integration architectures, namely loosely coupled and tightly coupled integration techniques in the following sections [6]. GPS and INS work individually in both integrations and the basic difference between these integrations is the type of data shared by both systems (GPS and INS) [6]. In loosely coupled technique, GPS raw measurements (pseudorange and Doppler observables) are processed through a kalman filter and then they are blended with INS computations but in tightly coupled technique, raw measurements from GPS are directly involved in the operation through a unique filter [2]. Both integrations are briefly explained in the next section.

5.0.4 Loosely Coupled Integration

The flow chart of loosely coupled integration is shown below. In loosely coupled

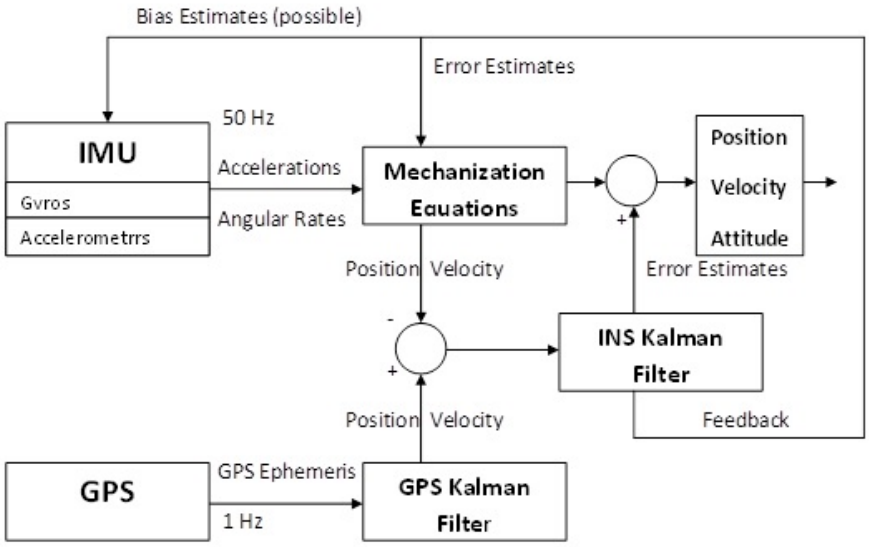

Figure 5.1: Loosely Coupled Integration Scheme.

integration systems, position, velocity and attitude measurements obtained from an INS are integrated with position, velocity and time measurements obtained from a GPS receiver. For this purpose, two kalman filters are used which operate independently of each other for GPS and INS measurements. We can call them GPS kalman filter and INS kalman filter. INS measurements are processed by INS kalman filter in order to provide PV (position, velocity) parameters while GPS raw measurements (code, Doppler and phase) are input to GPS kalman filter in order to

provide PV parameters which are further used as input to INS kalman filter. This filter determines the error estimates by calculating the difference between the both PV parameters generated by the GPS kalman filter and mechanization equations. These error estimates are further used as feedback to update the PV parameters from mechanization equations. Both kalman filters can support bias estimates for both inertial sensors (accelerometers, gyroscopes) as well. This feedback can compensate the known error [26].

5.0.5 Tightly Coupled Integration

The flow chart of tightly coupled integration is shown below.

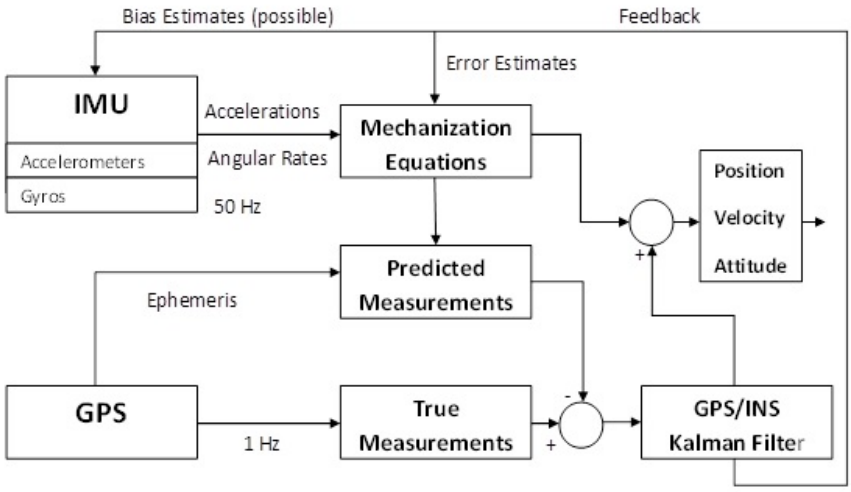

Figure 5.2: Tightly Coupled Integration Scheme.

In tightly coupled navigation systems, acceleration and angular rate measurements obtained from an INS are integrated with pseudorange and Doppler measurements obtained from GPS receiver. For this purpose, only a single kalman filter is used which may be called as GPS/INS kalman filter. INS measurements are processed by mechanization equations in order to provide PV parameters. These PV parameters together with raw GPS ephemeris are used to predict pseudorange and Doppler measurements. These predicted values are used as input to the kalman filter. The kalman filter determines the error estimates of PV parameters by taking the difference between the predicted pseudorange and Doppler measurements and the raw GPS pseudorange and Doppler measurements. These error estimates are further used to update the PV parameters obtained from mechanization equations

in order to get the PVA (Position, Velocity and Time) parameters of the state vector [26].

5.0.6 Loosely Coupled VS Tightly Coupled

Simple implementation and robustness is the main advantage of loose integration. The other advantages are faster processing time and reduced number of computations because PV parameters are used to update INS data which may also be obtained from other sources [18]. Two main disadvantages are [26].

- GPS filter fails to provide the measurement updates when the GPS signal quality is poor.
- Process noise must be added to the both filters since both are working independently. This type of filter operation is a function of SNR (signal-to-noise ratio) and as the SNR is decreased the system performance is reduced [2].

This integration is also known as decentralized integration since two kalman filters are used [26].

On the other hand, the main advantage of the tight integration is that it is still possible to update the INS even in the poor GPS signal quality because of the use of predicted and raw pseudorange and Doppler measurements. The disadvantage is that the size of the state vector increases because only one kalman filter is used which results in longer processing time. This integration is also known as centralized integration since only a single kalman filter is used [26].

Besides the reliability and robustness, the GPS/INS integrated solution delivers improved availability, superior short-term and long-term accuracies and higher data transmission rate than either of the individual systems [20]. The loosely coupled scheme will be implemented in this thesis work.

5.0.7 Implementation Methods

Both of the integration techniques may be implemented by using closed loop (feedback) or open loop (feed forward) approaches which are independent of each other . In closed loop approach, either an INS kalman filter (in case of loose integration) or an GPS/INS kalman filter (in case of tight integration) as a feedback is used to compensate all the estimated and misalignment errors which result small errors propagated by the mechanization equation [2]. In open loop approach, the job of the kalman filter is to estimate the sensors biases, correct them and output them and thus no information is sent back for compensation. In this way mechanization error introduces a fast growing error into the integrated system . This approach is good for high end inertial sensors since they produce small errors but in case of

low cost MEMS technology large errors are propagated in short periods of time and therefore there must be a feedback in order to compensate the mechanization parameters. For this reason we have to implement closed loop method in our case since we will use low cost MEMS technology.

We can consider the GPS/INS integration as two stages. The first stage concerns with the initial position of the vehicle which is static. The second stage concerns with the movement of the vehicle which is a dynamic system. The orientation of the vehicle is initialized by applying ZUPT (Zero Velocity Update) when the vehicle stops for some time (before it starts moving and jumps to the dynamic state).

5.1 The Kalman Filter: Introduction

The measurements taken by inertial sensor is noisy data. The main problem is to separate the signal from the noise which is an additive combination of the noise and signal itself. These measurements and system dynamics needs to be optimized in order to extract the precision in the data. For this purpose R. E. Kalman (1960) used the state-space technique to formulate the minimum mean-square error (MMSE) filtering problem. This algorithm is based on the two main features [21][3].

1. A vector model of a random process under some assumptions.
2. Recursive processing of the noisy data.

Generally it is believed that the kalman filter provides optimal solution of the navigation quantities depending on the model accuracy of a dynamic system [20].

5.2 The Discrete Kalman Filter

In practice usually all the strapdown inertial navigation systems are incorporated by a kalman filter. A discrete kalman filter is an efficient recursive solution for a discrete data set. Basically a kalman filter connects the system dynamics by estimating the state of a system and then comparing it with the system information already known by using the kalman gain matrix. Kalman gain matrix is introduced to weight. It gives us information about the relative uncertainty between the measurements and the current state estimate and then decides how much of the new observations can participate in the existing system. The filter will put more weight on the measurements when the gain is high but it will put more weight on the prediction model in case of low gain. In this case the noise will be smoothened but the response of the system will be decreased [4].

A discrete-time process may occur in two different ways, either in discrete steps such as random-walk problem or by sampling a continuous time process by using an ADC (Analog to Digital Converter) processor which changes an analog input signal to the digital signal [2]. The overall mathematical description of the kalman filter may be described by the following two models.

5.2.1 Dynamic Model

Dynamic model describe the transformation of the state vector over time. The dynamic equation of a continuous process may be written as

$$\dot{x} = Fx + Gu \tag{5.1}$$

Where x represents the state vector, F represents the dynamic matrix and G (design matrix) represents a vector which contains the coefficients of the input white noise. u is the forcing vector function. Usually the strapdown inertial navigation systems are implemented with the help of high-rate sampled data, therefore the dynamic equation needs to be transformed in its discrete time domain [14].

The dynamic model or the difference equation for a controlled discrete-time process can be written in the following way

$$x_{k+1} = \phi_k x_k + \omega_k \tag{5.2}$$

Where x_k is n dimensional state vector of the system at time t_k which contains the variable of interest (position and velocity). Basically our state vector will represent the degrees of freedom and dynamics of the system [38]. ϕ represents the state transition matrix which is derived from the dynamics matrix F of the dynamics model. It transforms any initial state to its corresponding state at time t. $_k$ is a vector of dynamic noise or the process noise in the system and it has predefined covariance.

There are always noise and imperfections in the system where we dont have control. But we need to deal with them as in the case of dynamic model or process model where we have to deal with the dynamic or the process noise which can be written

$$Q_k = E[\omega_k \omega_k^T] \tag{5.3}$$

Where the dynamic noise is

$$\omega_k = \int_{t_k}^{t_{k+1}} \mu(\epsilon) d\epsilon \tag{5.4}$$

Q_k is the dynamic or the process noise covariance matrix which may vary with each time step [22]. Q_k is determined by first order approximation of the state

transition matrix. In case of low cost inertial systems, Q_k must be selected in such a way that the stability of the filter is not affected and the trajectory can follow the GPS [14].

5.2.2 Observation Model

Observation model describes the linear relationship between the state and the measurements. In other words it describes the behavior of the vehicle. Since the measurements are occurring at discrete points in time, so we can write the observation model as follows.

$$z_k = H_k x_k + \upsilon \tag{5.5}$$

z_k denotes the actual measurements of variable x at time t. H_k is the observation matrix which is a relation between the state and the measurements z_k [22]. v_k is the random measurement error and is assumed to be the measurement noise or the white noise with its predefined covariance which has zero-cross correlation with the process noise. The measurement noise covariance is denoted by R_k and written as

$$R_k = E[\upsilon_k \upsilon_k^T] \tag{5.6}$$

The noise covariance matrices Q_k and R_k are considered to be uncorrelated.

5.3 Kalman Filter Algorithm

The functionality of a discrete kalman filter in the form of a loop is shown in the diagram below. The filter functions in the following two steps,

- Prediction
- Correction

The dynamic model is used to predict the system state in the first step. The second step is used to correct the state by using the observation model and hence the error variance is minimized which makes the filter an optimal filter. Because the process is repeated and updated thats why the filter is also called a recursive filter [38]. The process and the measurement noise require to be modeled before we implement the recursive algorithm to a random process. The basic kalman filter loop may be written in the following mathematical description [4]. Time update

$$\tilde{x}_{k+1} = \phi_k \hat{x}_k \tag{5.7}$$

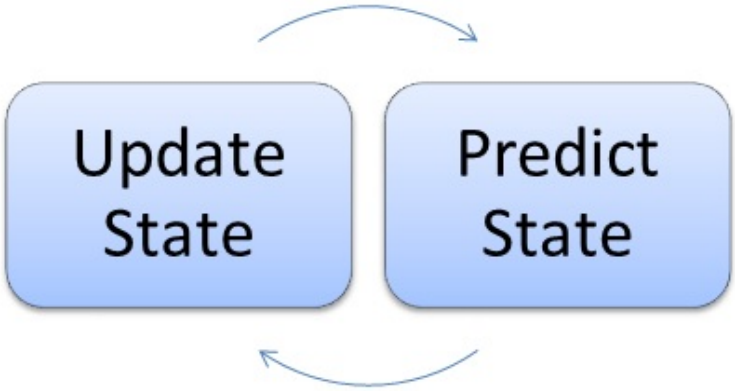

Figure 5.3: Discrete kalman filter cycle.

$$\tilde{P}_{k+1} = \phi_k \hat{P}_k \phi_k^T + Q_k \tag{5.8}$$

Measurement update

$$K_k = \tilde{P}_k H_k^T (H_k \tilde{P}_k H_k^T + R_k)^{-1} \tag{5.9}$$

$$\hat{x}_k = \tilde{x}_k + K_k(z_k - H_k \tilde{x}_k) \tag{5.10}$$

$$\hat{P}_k = (I - K_k H_k)\tilde{P}_k \tag{5.11}$$

Where K_k is the kalman gain matrix. Generally the following filter parameters are needed to be determined

- Transition matrix ϕ
- Process noise Q
- Design matrix H
- Measurement noise R
- Initial conditions $\tilde{x}_0 \tilde{P}_0$

Equations (5.7) and (5.8) are known as time update equations or predictor equations while Equations (5.9), (5.10) and (5.11) are known as measurement update equations or corrector equations [22]. There are number of techniques to implement a kalman filter but theoretically they are the same techniques. Some of the techniques may be less complex than the others [13].

5.3.1 Calculation of matrices involved in the kalman filter design

Numerical approximation for different matrices involved in the kalman filter design is added in this section. All the matrices are written in one dimension. Later in the Matlab code, these matrices are spread to three dimensions by using the in-built Matlab function kron (kronecker tensor product) . In the observation model, our 3D state vector consists of 12 states as given below.

$$x = [p_x, v_x, \text{psi}_x, g_x, p_y, v_y, \text{psi}_y, g_y, p_z, v_z, \text{psi}_z, g_z] \tag{5.12}$$

Where,

$$g_b = [\text{gyrox}_{bias}, \text{gyroy}_{bias}, \text{gyroz}_{bias}] \tag{5.13}$$

$$psi = [roll, pitch, yaw] \tag{5.14}$$

phi is the state transition matrix which connects the state vector from time k to $k+1$ and it can be calculated by the following numerical approximation.

$$\phi = exp(F.\Delta t) \approx I + F.\Delta t \tag{5.15}$$

$$\phi = \begin{bmatrix} 1 & dt & 0 & 0 \\ 0 & 1 & 0 & 0 \\ 0 & 0 & 1 & dt \\ 0 & 0 & 0 & 1 \end{bmatrix} \tag{5.16}$$

Process noise matrix can be written as

$$Q = \begin{bmatrix} q_v\frac{\Delta t^3}{3} & q_v\frac{\Delta t^2}{2} & 0 & 0 \\ q_v\frac{\Delta t^2}{2} & q_v\Delta t & 0 & 0 \\ 0 & 0 & q_g\frac{\Delta t^3}{3} & q_g\frac{\Delta t^2}{2} \\ 0 & 0 & q_g\frac{\Delta t^2}{2} & q_g\Delta t \end{bmatrix} \tag{5.17}$$

Covariance matrix R for the observations can be written as

$$R = \begin{bmatrix} \sigma_p^2 & 0 \\ 0 & \sigma_g^2 \end{bmatrix} \tag{5.18}$$

Design matrix H can be written as

$$H = \begin{bmatrix} 1 & 0 & 0 & 0 \\ 0 & 0 & 0 & 1 \end{bmatrix} \tag{5.19}$$

Observation vector z can be written as

$$z = \begin{bmatrix} p_x - \tilde{p}_x \\ g_x - \tilde{g}_x \end{bmatrix} \tag{5.20}$$

Chapter 6

Vehicular Mission, Test Results and Analysis

This chapter is composed of two main sections. The mission details, system hardware configuration and equipment used are described in the first section while the results obtained from the mission are analyzed in the second section of the chapter.

6.1 Mission Details

In this section the physical configuration of the system and the mission details have been discussed. In the vehicle tracking navigation both the highway and city tracking is included. The navigation started on 6th of September 2011. The navigation starting point was the parking area of UMB (UNIVERSITETET FOR MILJ- OGBIOVITENSKAP/NORWEGIAN UNIVERSITY of LIFE SCIENCES) and ending point was Oslo city. UMB is situated in s Kommune which is approximately 34 km from city Oslo. A screen shot of the whole route from Google Earth is shown in the figure 6.1. The yellow pointer shows the UMB parking area. The mission started at 09:11 according to GPS time clock and ended at 11:51. The total navigation was done for 2 hours and 40 minutes.

6.2 The System Hardware Setup

The type of vehicle used for the mission was FORD TRANSIT CONNECT as shown in the figure 6.2. A navigation grade IMU of the type HG9900 IMU from Honeywell has been used in this mission in order to record the angular rates and accelerations and the calculated positions on the basis of these measurements will

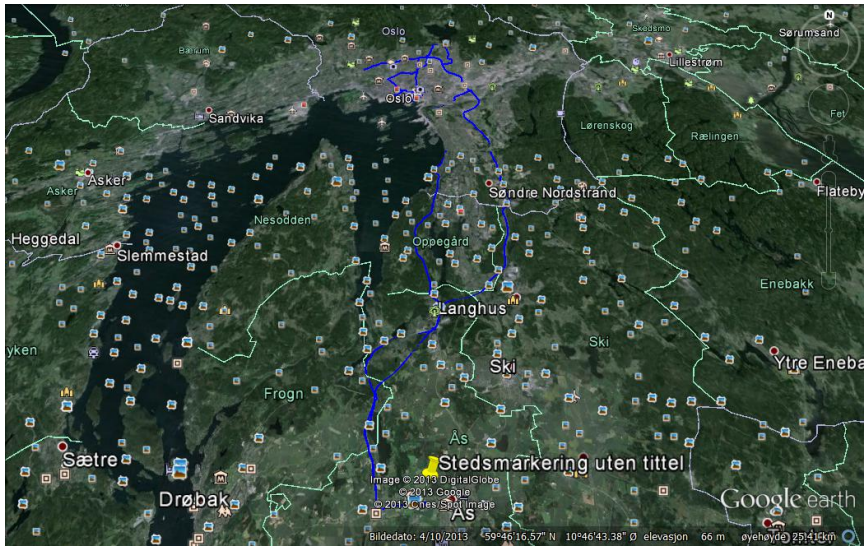

Figure 6.1: Mission map drawn from Google Earth [4]

be further used as references. It can provide precise and independent position information for the navigation purpose. This is a small, lightweight and low power consuming device capable of operating across the spectrum of irregular and rough environments [16]. This IMU includes high end digital laser gyros of the type GG1320AN and accelerometers of the type QA2000. The key characteristics of these inertial sensors are given in the table 5.1. Further details about the system characteristics and specifications can be found in the Appendix B The IMU and three GPS receiver antennas for navigation measurements are mounted on the roof of the vehicle while the rest of the system electronics was installed inside the vehicle.

HG9900 IMU	Accelerometer	Gyroscope
Error Coefficient	1σ	1σ
Bias Stability	$< 25\mu g$	0.003 deg/hr
Scale Factor	$< 100PPM$	$< 5.0PPM$
Random walk		$< 0.002deg/hr$

Table 6.1: HG9900 IMU Characteristics

Figure 6.2: Vehicle used for mission [4]

6.2.1 IMU

A low-end IMU and a low-cost GPS receiver have been mounted on the OBU (On Board Unit) device which is installed on the dashboard of the vehicle. Both accelerometers and gyroscopes used inside this IMU are MEMS type with digital output. These inertial sensors are explained briefly in the following subsections [17].

LIS331DLH 3-axis accelerometer

A high performance three axes linear accelerometer of the type LIS331DLH has been used which belongs to nano family. This is an ultra low-power device which offers zero-g level, self-test and sleep to wake-up functions. For example the functionality of the sensor can be checked by self-test without any movement of the sensor. In sleep mode the device is still observing the acceleration but consuming the less power [17]. LIS331DLH is widely used in many applications such as intelligent power saving devices, vibration monitoring and compensation etc. Further details about LIS331DLH accelerometer can be found in the Appendix A.

L3G4200D digital gyroscope

A low-power three axes ultra-stable gyroscope of the type L3G4200D has been used in the IMU. This gyro is capable of providing stable zero rate level and is ultra-stable over temperature and time [17]. L3G4200D gyro is used in many applications such as GPS applications and robotics etc. Further details about the gyro can be found in Appendix A.

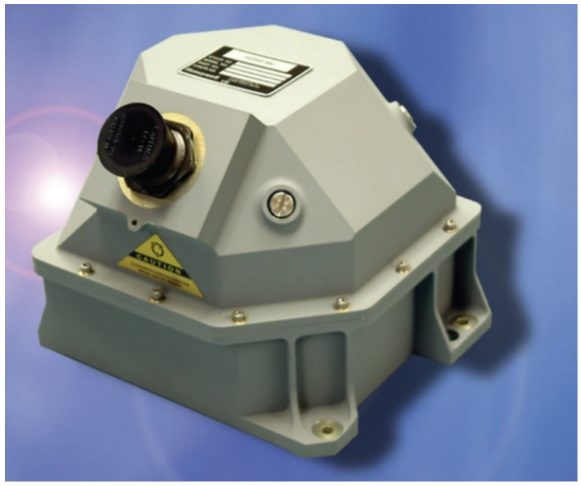

Figure 6.3: Honeywell HG9900 IMU [16]

6.2.2 Sensor positions and orientation

Both the accelerometer and the gyro are detecting the accelerations and angular rotations respectively in their own predefined directions given by the manufacturers. These sensors are mounted in the opposite directions in the unit as shown in the figure. 6.6. Therefore they need to be aligned with the vehicles coordinate axes. This alignment has been considered in the Matlab program.

6.2.3 System Coordinates

The coordinates are given in the same coordinate system as GNSS/INS-frame. Points 1-3 in the table are known points in GNSS/INS-frame. Point 4th is the Q-free device (code receiver) and 5th is the high-end sensor (IMU). More details about the vehicle coordinates can be seen in Appendix D.

6.2.4 Data Collection

The data used in the results was collected in a vehicle in a mixed environmental scenario starting from s kommune, Norway which is approximately 34 kilometers from the capital city Oslo as mentioned earlier in the previous section. This mixed environment consists of a highway and a typical downtown urban scenario which is characterized by difficult operational environment because of the signal blocking and multipath in the tunnels and typical downtown environment consisting of high buildings, traffic lights, pedestrian crossings and traffic jams.

Figure 6.4: 3-axis MEMS accelerometer [17]

Figure 6.5: 3-axis MEMS gyroscope [17]

The road trip starts in a parking area of UMB and continues on a highway (E 18) where it passes some tunnels and then further continues into the core downtown environment where the number of available satellites is definitely reduced. To way back to UMB, vehicle takes another route (E 6) as shown in the figure 6.1, and finishes in the same parking area. But this return trip has not been included in the test analysis since we dont have available data for this time slot. The total time taken by the vehicle is about 2 hours and 40 minutes which includes some stops due to traffic signals, traffic jams, pedestrian crossings and mission planning time intervals. The speed of the vehicle varies approximately from 0 to 80 km/h.

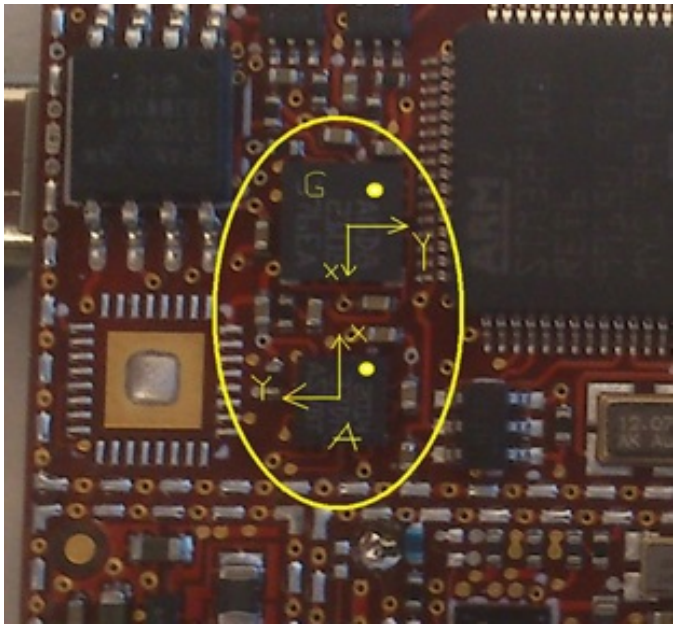

Figure 6.6: : Inertial sensors orientation in the OBU [4]

6.2.5 Data Processing

The navigation data is continuously stored on the computer installed inside the vehicle. The IMU is connected to the computer via Ethernet. The stored data is a text file type. The GPS measurements are stored in the GPS receiver as a log file. An example of these data files can be seen in the Appendix D.

6.3 Results and analysis

In this section, our main focus will be on the operational environment, test results and analysis. The results obtained by the high end sensors, demonstrating the partial and long term data outages. Position accuracy and challenging operational environments are included in this section. For this purpose, a navigation grade HG9900 IMU consisting of MEMS-based high-end inertial sensors has been used as mentioned earlier in the previous section. This unit is used for measuring the true positions and the results provided by the unit are used as references for comparison since they are based on precise and independent navigation information. On the other hand, a prototype low end sensor from Q-free is installed on the dashboard of the vehicle. This unit provides us an GPS/IMU (INS) integrated navigation solution and the results obtained from this unit are then compared with the

reference results obtained by post-processing procedures to analyze the behavior of the low cost MEMS-based measurement unit. For this purpose, loosely coupled strategy has been adopted where GPS/IMU integrated results are considered both with and without kalman filter implementations.

The GPS positioning update frequency is 1 Hz and IMU is updating at 50 Hz which means for each GPS update, 50 IMU updates are available. Thus the time interval must be synchronized before integrating the both systems. This synchronization has been done in the Matlab code which is shown in appendix (). The reference trajectory performed by using high end sensors will be compared with the integrated solution of GPS and IMU. Then a kalman filter will be implemented for the integration purpose which will provide a filtered solution for comparison.

6.3.1 The Raw IMU Data

First of all we will start looking the behavior of low cost IMU ($Q-free$ device) by plotting the raw data received from IMU. The raw accelerometer measurements are taken during the whole vehicle mission. These measurements were taken in milliG but converted into m/s^2 before they were used in the navigation process. Figure

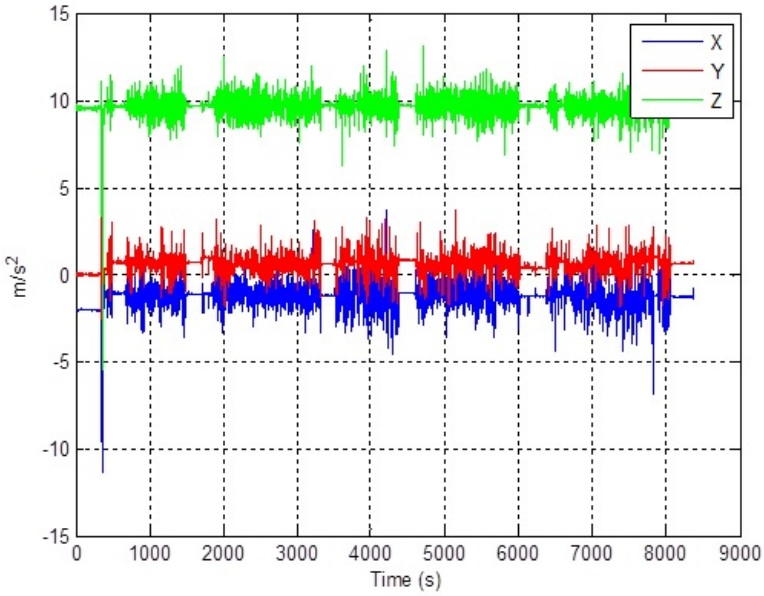

Figure 6.7: Accelerometer raw measurements

6.7 displays the unchanged raw measurements of the accelerometer along x, y, and

z-axis. The behavior of the accelerometer is quite understandable since the plotted measurements along z-axis are just close to 9.81 and acceleration measurements along x, and y-axis, are just the small variations around zero.

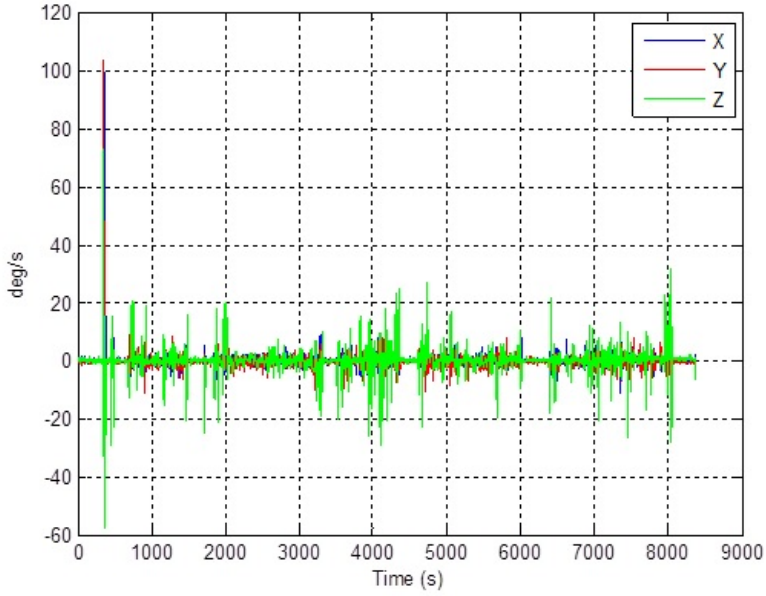

Figure 6.8: Gyroscope raw measurements

The Figure 6.8 displays the unchanged gyroscope measurements. A constant bias is present in these measurements. These measurements are taken by the IMU in milli Degrees Per Second but they are converted to rad/sec before their use in navigation process.

6.3.2 Satellite visibility

The satellite visibility of reference data has been very good during the vehicular mission time. The average number of satellite vehicles been around 7 throughout the mission and a minimum number of 4 satellite vehicles were available all the time as shown in the Figure 6.9.

6.3.3 Positioning Error

The position estimates based on the GPS measurements depend on the errors in the measurements. Position estimate is assumed to be worse in case of larger error in the measurements and it may be improved in case of increased number of satellites

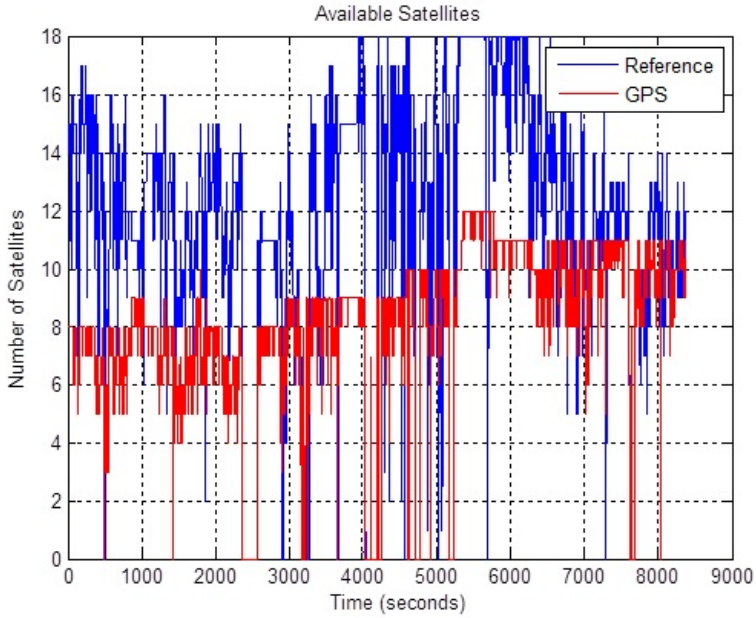

Figure 6.9: Satellite visibility

in view which may be considered as second assumption. But even if the number of satellites increases, there is no guarantee that the position will be improved. This is because there is no linear relationship between the current and previous positions which reveals the fact that the satellite geometry is also very important to consider. At this level we are interested in position in geographical frame (local frame), so we are interested in the horizontal error which can be found by the following formula [25].

$$\textbf{RMS horizontal error} = (\sigma_E^2 + \sigma_N^2) = \sigma + HDOP \tag{6.1}$$

Where σ is the standard deviation and HDOP horizontal DOP (Dilution of Precision). Actually user-satellite geometry is provided by the DOP values. A higher DOP value means a weak geometry and a lower DOP and $+sigma$ can produce a better position estimate. This concept will be more cleared in the test analysis.

We have chosen three different scenarios in order to analyze the results.

1. Motorway Scenario
2. Tunnels Scenario
3. City Centrum Scenario

Scenario 1: Motorway

In this scenario we have chosen a time slot of 300 hundred seconds on motorway (E 18). The horizontal position in meters has been shown in the Figure 6.10 below. The Trajectory shows the clear difference between the INS and the filtered solution

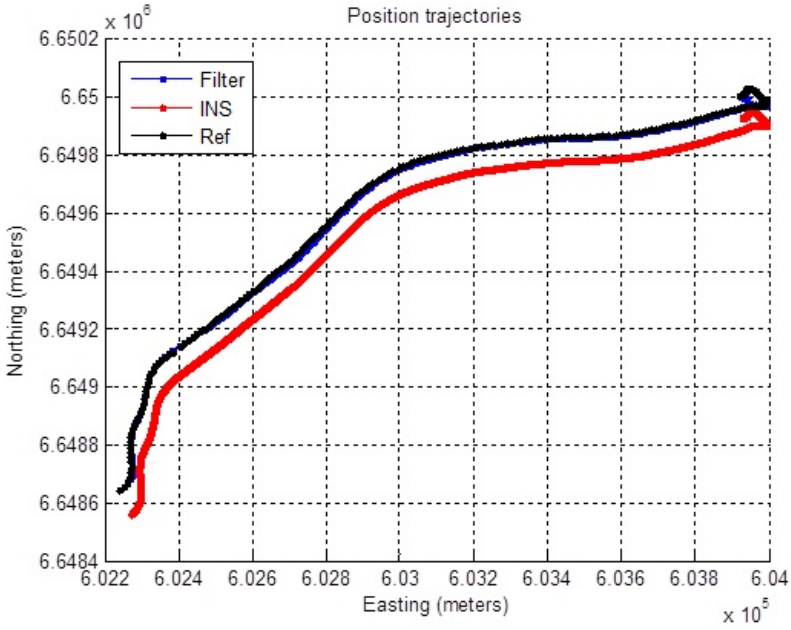

Figure 6.10: Position (g-frame) scenario 1.

through the kalman filter. The filter solution is following the reference trajectory very smoothly. The 2D horizontal position error has been shown for the same time slot. Here the error is around 10 meters from 600 to 800 seconds but it starts increasing right after 800 seconds. This can be compared with the number of available satellites at that time which has been reduced to 5 and 9 for GPS and Reference data.

Scenario 2: Opera Tunnel

The Opera Tunnel has been chosen as a second scenario. It starts at 9:13:40 and ends at 9:17:08 which means its a 208 seconds time slot. The trajectory for this time slot has been shown in the figure below. No GPS signals are available in the tunnel. The INS solution just initializes itself with the GPS position after passing the tunnel. The 2D error increases abnormally for that time slot as shown in the Figure 6.14. There is no satellite available for this time slot which is the reason for

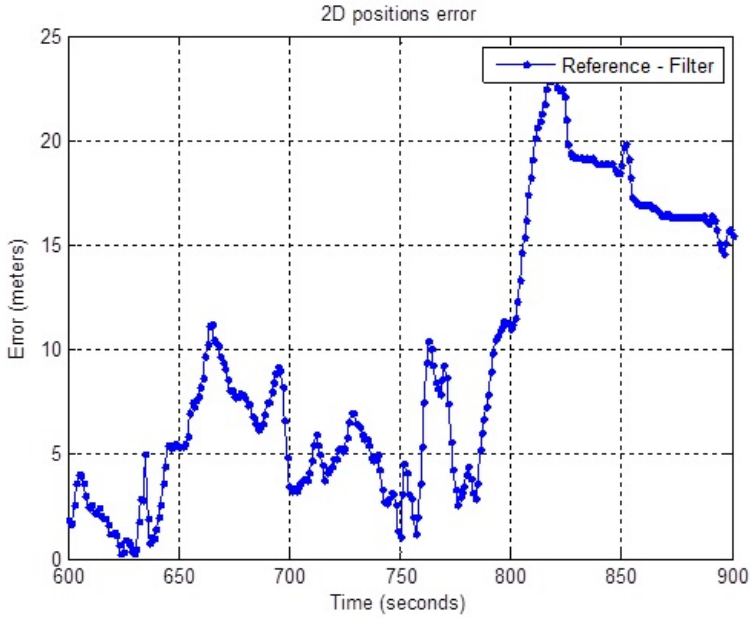

Figure 6.11: Position Error (Reference-filter) scenario 1.

this large error.

Scenario 3: City Centrum

The third and last scenario has been chosen the downtown area of Oslo city.

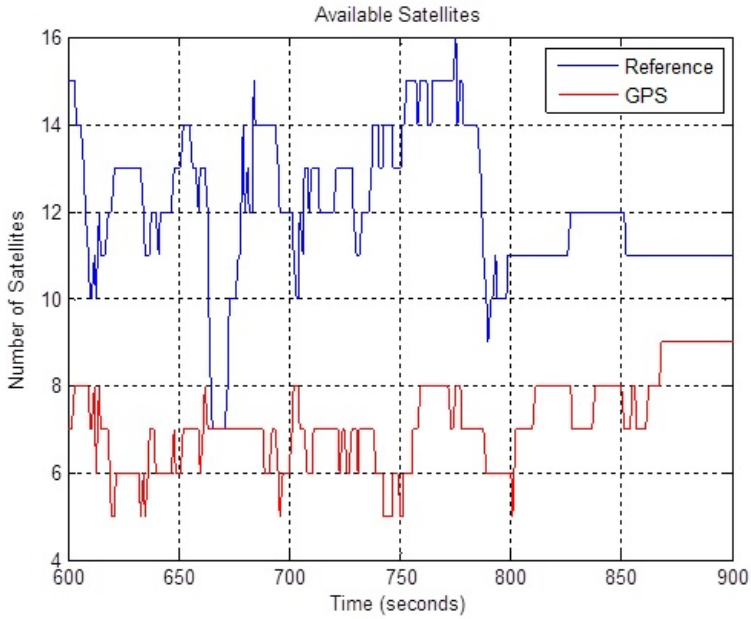

Figure 6.12: Satellite visibility scenario 1.

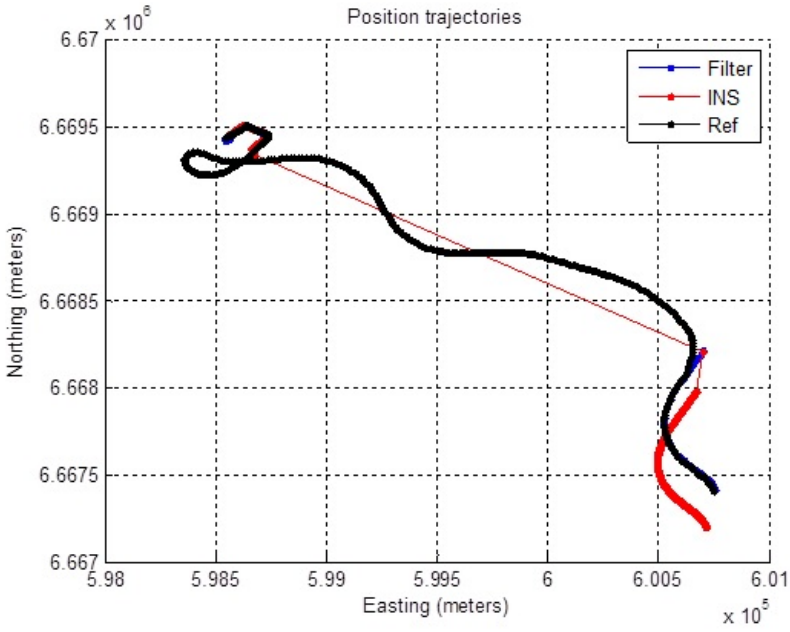

Figure 6.13: Position (g-frame) scenario 2.

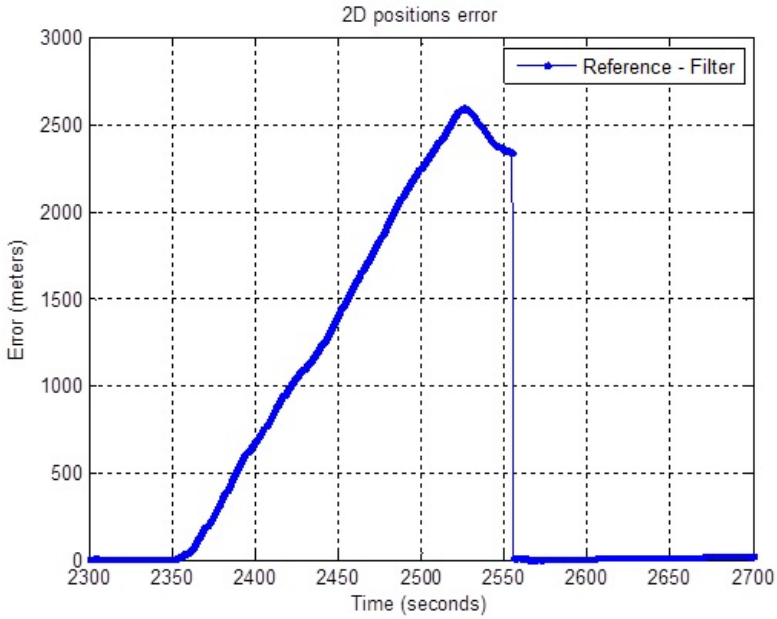

Figure 6.14: Position Error (Reference-filter) scenario 2.

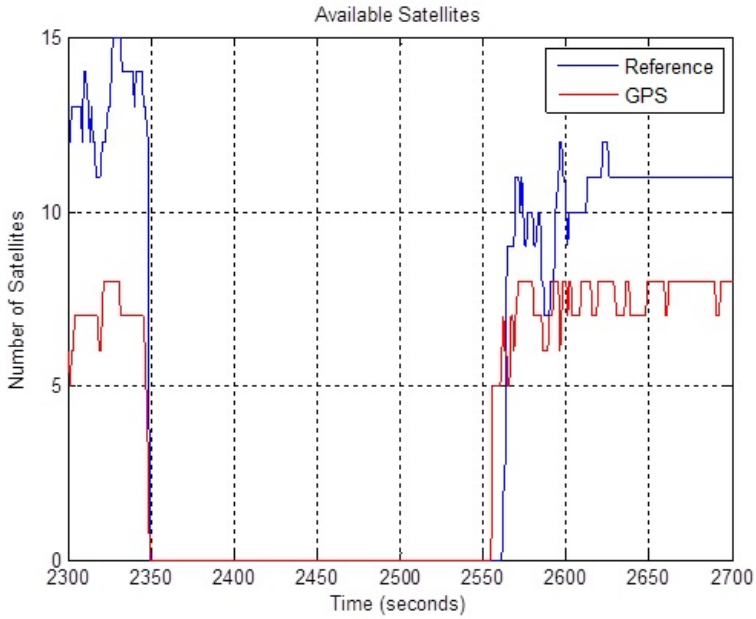

Figure 6.15: Satellite visibility scenario 2.

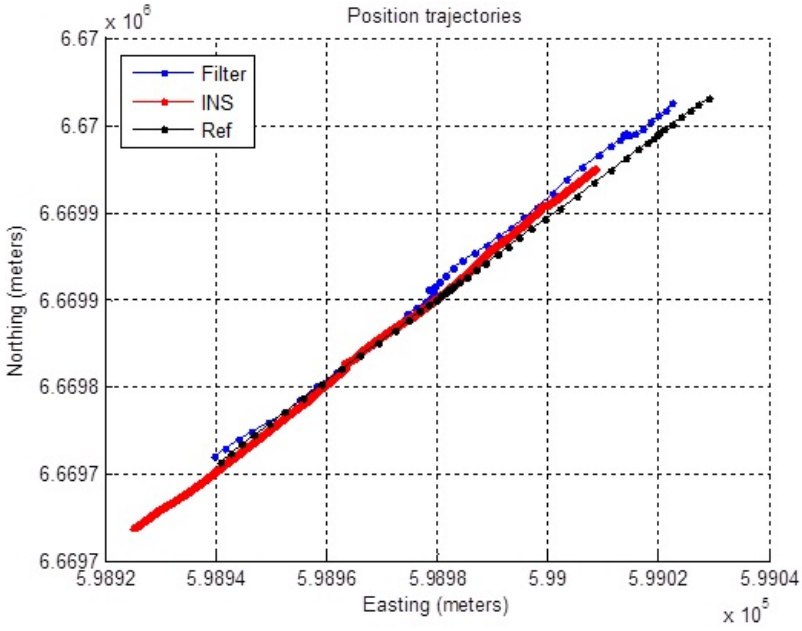

Figure 6.16: Position (g-frame) scenario 3.

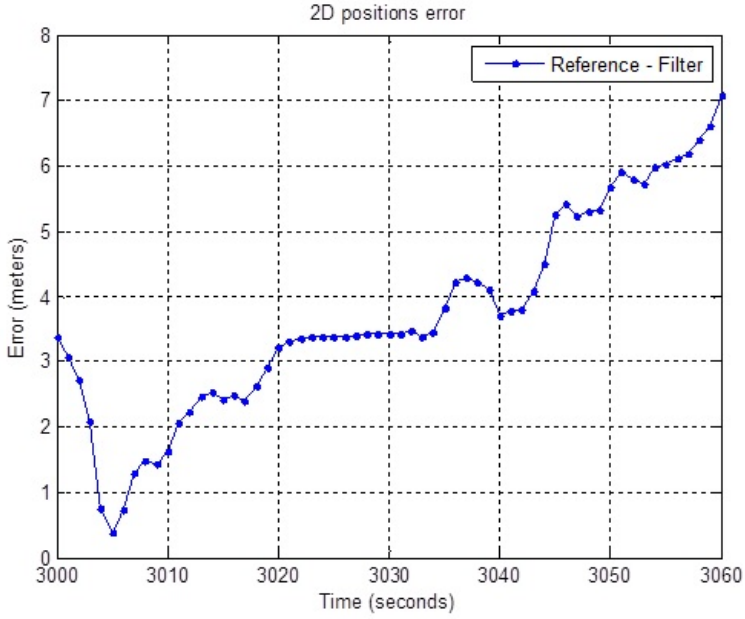

Figure 6.17: Position Error (Reference-filter) scenario 3.

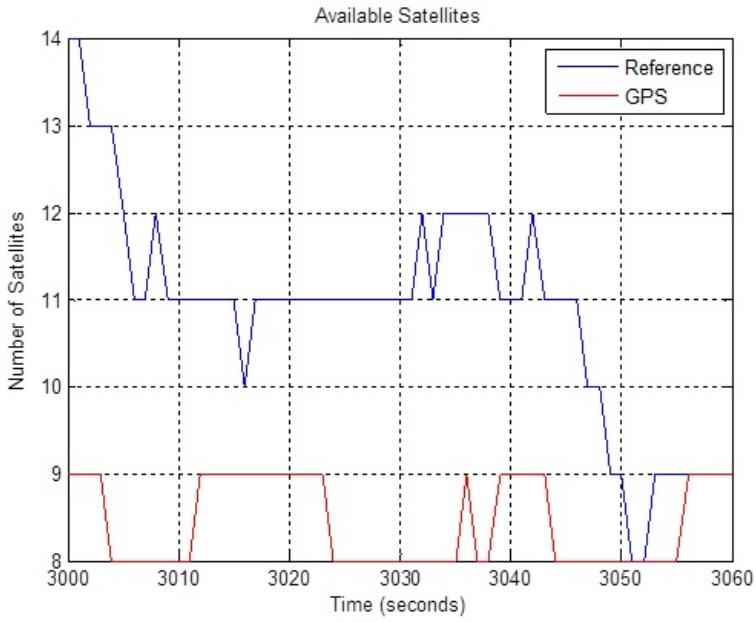

Figure 6.18: Satellite visibility scenario 3.

Chapter 7

Summary, conclusions and recommendations

7.1 Summary and conclusions

The main objective of this thesis work was to analyze the performance of a low-cost MEMS based INS for vehicular applications especially in urban areas where the GPS signal quality is degraded. The behavior IMU has been checked and analyzed, how does it functions. After that it has been compared with the reference positions measured by high end sensors on the vehicle. The Russian satellite system GLONASS was combined with American GPS in order to increase the number of satellites available. A low-cost MEMS based IMU from Honeywell HG9900 and a GPS/GLONASS receiver were used as main equipment. Tightly coupled integration has been used for high-end sensors in order to produce reference data while loosely coupled integration has been used for low cost GPS/IMU integration. In the end 2D horizontal position error has been calculated in order to compare the reference (true) positions with the filtered solution to see the position accuracy of the system. Accelerometers were measuring the acceleration and gyros were measuring the rotational rates but their participation wss not enough. Quality of accelerometers is not good and gyros tend to drift a lot. Kalman filter measures the velocity. But if we want velocity, we have to integrate twice which will make the accelerometer measurements better. But if we are able to measure the velocity from an external sensor then we need integration just once. The results shows that the performance of an GPS/IMU integrated system is much better than the only GPS or only IMU. We have seen in the test results section when we pass through the tunnel the satellite signal vanishes. On the other hand the high

end sensor is mounted on the roof of the vehicle but low cost sensor is mounted inside the vehicle which possibly can experiences a bad user-satellite geometry. We know that the number of satellite is not the guarantee for a good position, the geometry of the satellites is also very important. Heading is an important component in order to estimate the position in advance. When the vehicle is running with some speed, the estimate of heading looks good. But as soon as the vehicle stops on a traffic light or the speed of the vehicle becomes very slow, the heading goes uncontrolled. In order to get the right orientation of the vehicle, ZUPT updates are applied. The accelerometers are still measuring the gravity component even if the vehicle has been stopped. This can help the system attitude. The problem may be solved if we would be able to get velocity somehow directly from the vehicle. The other solution for the heading may be a compass but this might not be very reliable solution due to magnetic mechanism of the compass which is used to be reduced when interacting with metals.

7.2 Recommendations

This thesis work introduces GPS/IMU integrated navigation solution performance in urban areas very briefly and only the RMS error has been analyzed to justification. Definitely, there is a lot of practical and theoretical research work which can be done to improve the quality of the technology and enhance the system performance by minimizing the errors. Some of the important issues are listed below

- The quality of the IMU sensors may be improved and different qualities of sensors may be tested. Different error models may also be introduced to the kalman filter.
- Other integration techniques may also be tested.
- An external sensor to measure the velocity can be used inside the vehicle. For example, an odometer can be used. A simple odometer is capable of counting the number of wheel rotations and if we know the perimeter of the wheel, the distance traveled can be found by multiplying it by the number of rotations and hence the velocity can be determined by simply dividing the perimeter by the it takes for each rotation. Another option may be an optical odometer, which is capable of measuring the distances without touching the surface.
- A magnetic compass may be used also be used in case of signal blockages. But this might not be a reliable solution because the quality of the compass will be degraded with the passage of time since it will interact with other metals.

- INS may be stopped during the signal blockages and initializes again as soon as the situation becomes normal in order to avoid the drift, especially gyros drift a lot which makes the INS unstable.

Bibliography

[1] https://www.wikipedia.org/.

[2] Saurabh Godha. Performance evaluation of low cost mems-based imu integrated with gps for land vehicle navigation application. *UCGE Report*, (20239), 2006.

[3] http://www.gps.gov/systems/gps/space/.

[4] J. G. O. Gjevestad. *Navigation Systems (TTT4150)*. Course Notes, NTNU, 2013.

[5] Haakon Ellingsen. *Development of a Low-Cost Integrated Navigation System for USVs*. Department of Engineering Cybernetics, NTNU, Trondheim, Norway, 2008.

[6] http://www.edi.lv/media/uploads/userfiles/navigationlondon.pdf.

[7] http://www.gdgps.net/products/tecmaps.html.

[8] http://iono.jpl.nasa.gov/latestrtiglobal.html.

[9] AD King. Inertial navigation-forty years of evolution. *GEC review*, 13(3):140–149, 1998.

[10] Aboelmagd Noureldin, Tashfeen B Karamat, and Jacques Georgy. *Fundamentals of Inertial Navigation, Satellite-Based Positioning and Their Integration*. Springer, 2013.

[11] Kenneth Gade. Introduction to inertial navigation. 2004.

[12] http://i1-news.softpedia-static.com/images/news2/mems-technology-allows-for-tiny-gyroscopes-2.jpg.

[13] Jay Farrell. *Aided navigation: GPS with high rate sensors*. McGraw-Hill New York, 2008.

[14] Eun-Hwan Shin and Naser El-Sheimy. *Accuracy improvement of low cost INS/GPS for land applications*. University of Calgary, Department of Geomatics Engineering, 2001.

[15] David Titterton, John Weston, et al. Strapdown inertial navigation technology. 2nd edition. *The Institution of Electronical Engineers, Reston USA*, 2004.

[16] www.honeywell.com.

[17] www.st.com.

[18] Mark G Petovello. *Real-time integration of a tactical-grade IMU and GPS for high-accuracy positioning and navigation*. 2003.

[19] Antonio Angrisano. Gnss/ins integration methods. *Published thesis (PhD),Parthenope University of Naples*, 2010.

[20] Steve Hewitson and Jinling Wang. Extended receiver autonomous integrity monitoring (e raim) for gnss/ins integration. *Journal of Surveying Engineering*, 136(1):13–22, 2010.

[21] Robert Grover Brown, Patrick YC Hwang, et al. *Introduction to random signals and applied Kalman filtering*, volume 3. John Wiley & Sons New York, 1992.

[22] Greg Welch and Gary Bishop. An introduction to the kalman filter, 1995.

[23] Borje Forssell. Radionavigation systems. 2008.

[24] http://www.novatel.com/assets/documents/manuals/om-20000008.pdf.

[25] Pratap Misra and Per Enge. *Global Positioning System: Signals, Measurements and Performance Second Edition*. Massachusetts: Ganga-Jamuna Press, 2006.

[26] Casper Ebbesen Schultz. *INS and GPS integration*. PhD thesis, Technical University of Denmark, DTU, DK-2800 Kgs. Lyngby, Denmark, 2006.

[27] David Russell. Integrating ins and gnss sensors to provide reliable surface positioning. pages 1–11, 2012.

[28] Muhammad Shafiq. *Ground Station Antenna. NUTS Student Satellite Project*. Department of Electronic and Telecommunication, NTNU, Trondheim, Norway, 2012.

[29] Richard B Langley. Dilution of precision. *GPS world*, 10(5):52–59, 1999.

[30] Jay Farrell and Matthew Barth. *The global positioning system and inertial navigation*, volume 61. McGraw-Hill New York, 1999.

[31] Oliver J Woodman. An introduction to inertial navigation. *University of Cambridge, Computer Laboratory, Tech. Rep. UCAMCL-TR-696*, 14:15, 2007.

[32] Yueming Zhao. Gps/imu integrated system for land vehicle navigation based on mems. 2011.

[33] Christopher Hide. *Integration of GPS and low cost INS measurements*. PhD thesis, University of Nottingham, 2003.

[34] Minha Park. *Error analysis and stochastic modeling of MEMS based inertial sensors for land vehicle navigation applications*. University of Calgary, Department of Geomatics Engineering, 2004.

[35] Minha Park and Yang Gao. Error and performance analysis of mems-based inertial sensors with a low-cost gps receiver. *Sensors*, 8(4):2240–2261, 2008.

[36] IEEE. Standard specification format guide and test procedure for single-axis laser gyros. 2006.

[37] Dr. Ing Zizung Yoon Dip. Ing. Karsten. *Introduction into quaternions for spacecraft attitude representation.* Department of Astronautics and Aeronautics, Technical University of Berlin, Germnay, 2012.

[38] Rachel Kleinbauer. Kalman filtering implementation with matlab. 2004.

Appendix A

L3G4200D

MEMS motion sensor: ultra-stable three-axis digital output gyroscope

Preliminary data

Features

- Three selectable full scales (250/500/2000 dps)
- I^2C/SPI digital output interface
- 16 bit-rate value data output
- 8-bit temperature data output
- Two digital output lines (interrupt and data ready)
- Integrated low- and high-pass filters with user-selectable bandwidth
- Ultra-stable over temperature and time
- Wide supply voltage: 2.4 V to 3.6 V
- Low voltage-compatible IOs (1.8 V)
- Embedded power-down and sleep mode
- Embedded temperature sensor
- Embedded FIFO
- High shock survivability
- Extended operating temperature range (-40 °C to +85 °C)
- ECOPACK® RoHS and “Green” compliant

Applications

- Gaming and virtual reality input devices
- Motion control with MMI (man-machine interface)
- GPS navigation systems
- Appliances and robotics

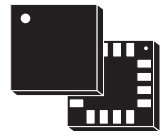

LGA-16 (4x4x1.1 mm)

Description

The L3G4200D is a low-power three-axis angular rate sensor able to provide unprecedented stablility of zero rate level and sensitivity over temperature and time. It includes a sensing element and an IC interface capable of providing the measured angular rate to the external world through a digital interface (I^2C/SPI).

The sensing element is manufactured using a dedicated micro-machining process developed by STMicroelectronics to produce inertial sensors and actuators on silicon wafers.

The IC interface is manufactured using a CMOS process that allows a high level of integration to design a dedicated circuit which is trimmed to better match the sensing element characteristics.

The L3G4200D has a full scale of ±250/±500/ ±2000 dps and is capable of measuring rates with a user-selectable bandwidth.

The L3G4200D is available in a plastic land grid array (LGA) package and can operate within a temperature range of -40 °C to +85 °C.

Table 1. Device summary

Order code	Temperature range (°C)	Package	Packing
L3G4200D	-40 to +85	LGA-16 (4x4x1.1 mm)	Tray
L3G4200DTR	-40 to +85	LGA-16 (4x4x1.1 mm)	Tape and reel

LIS331DLH

MEMS digital output motion sensor ultra low-power high performance 3-axes “nano” accelerometer

Features

- Wide supply voltage, 2.16 V to 3.6 V
- Low voltage compatible IOs, 1.8 V
- Ultra low-power mode consumption down to 10 µA
- ±2*g*/±4*g*/±8*g* dynamically selectable full-scale
- I^2C/SPI digital output interface
- 16 bit data output
- 2 independent programmable interrupt generators for free-fall and motion detection
- Sleep to wake-up function
- 6D orientation detection
- Embedded self-test
- 10000 *g* high shock survivability
- ECOPACK® RoHS and “Green” compliant (see *Section 8*)

Applications

- Motion activated functions
- Free-fall detection
- Intelligent power saving for handheld devices
- Pedometer
- Display orientation
- Gaming and virtual reality input devices
- Impact recognition and logging
- Vibration monitoring and compensation

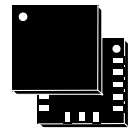

LGA 16 (3x3x1 mm)

Description

The LIS331DLH is an ultra low-power high performance three axes linear accelerometer belonging to the “nano” family, with digital I^2C/SPI serial interface standard output.

The device features ultra low-power operational modes that allow advanced power saving and smart sleep to wake-up functions.

The LIS331DLH has dynamically user selectable full scales of ±2*g*/±4*g*/±8*g* and it is capable of measuring accelerations with output data rates from 0.5 Hz to 1 kHz.

The self-test capability allows the user to check the functioning of the sensor in the final application.

The device may be configured to generate interrupt signal by inertial wake-up/free-fall events as well as by the position of the device itself. Thresholds and timing of interrupt generators are programmable by the end user on the fly.

The LIS331DLH is available in small thin plastic land grid array package (LGA) and it is guaranteed to operate over an extended temperature range from -40 °C to +85 °C.

Table 1. Device summary

Order codes	Temperature range [° C]	Package	Packaging
LIS331DLH	-40 to +85	LGA 16	Tray
LIS331DLHTR	-40 to +85	LGA 16	Tape and reel

Appendix B

HG9900 IMU

PROVIDING NAVIGATION-GRADE PERFORMANCE WITH PROVEN INERTIAL SENSOR TECHNOLOGY IN A SMALL, LIGHTWEIGHT PACKAGE TO MEET THE EVOLVING NEEDS OF OUR AEROSPACE CUSTOMERS

System Features

Inertial Measurement Unit (IMU)

- Honeywell GG1320AN Digital Laser Gyros
- Honeywell QA2000 Accelerometers
- Honeywell Smart Inertial Electronics
- Proven 0.8 nmi/hr performance

IMU Processor

- TI DSP TMS320VC33 (60 Mips)
- 128 Kbytes SRAM, 512 Kbytes Flash EEPROM

Standard I/O

- SDLC RS-422
- 300 Hz filtered angular rate and linear acceleration (other frequencies available)
- 300 Hz compensated ΔVs and $\Delta\Theta$s (other frequencies available)

Power Input

- 5, ±15 Vdc input

System Characteristics

Size

- < 103 cubic inches (5.5 x 6.4 x 5.34" including connector & mounting holes)

Power Requirement

- < 10 watts

Weight

- < 6.5 lbs.

Thermal Operating Range

- -54°C to +71°C

Gyro

Error Coefficients (1 Sigma)

- Bias: <0.003 deg/hr
- Random Walk: <0.002 deg/√hr
- Scale Factor: <5.0 PPM

Accelerometer

Error Coefficients (1 Sigma)

- Bias: <25µg
- Scale Factor: < 100 PPM

HG9900 IMU

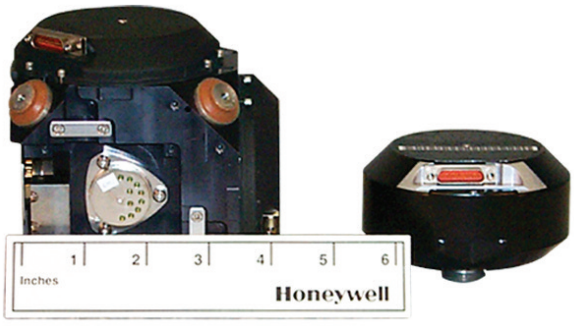

NAV100™ ISA

RLG

Find out more

For more information contact us by phone at 1-727-539-4130.

Honeywell Aerospace
1944 East Sky Harbor Circle
Phoenix, AZ 85034
800-601-3099
International: 602-365-3099
www.honeywell.com

Honeywell

N61-0491-000-001
September 2009

Appendix C

Geodetic coordinates

A consistent model of the shape of the Earth is needed since the geoid is only the approximation of the ellipsoid [16]. The gravitational and the centrifugal forces make the gravity vector. The centrifugal force is maximum near the equator and zero along the rotational axis of the Earth. The gravity vector is normal to the geodetic surface which is different from the actual surface of the Earth. The actual surface of the Earth fluctuates with respect to the geoid which is defined as the average sea level of the Earth. When an ellipse rotates around its minor axis, it forms an ellipsoid. The origin of the ellipsoid is the Earth's center of mass. The coordinates of the ellipsoid are called geodetic coordinates and they are latitude, longitude and geodetic height ($\emptyset, \lambda \; and \; h$ respectively). WGS84 geodetic system will be used throughout this study work. This system is defined by four parameters which are equatorial radius (semiminor axis), reciprocal flattening, Earth's rotation rate and gravitational constant [16].

ECEF reference frame Transformations

Here we will discuss the transformation between the rectangular and the geodetic coordinates. First we can define the WGS84 parameters.

$$Semimajor\ axis: a = 6378137\ m$$

$$Reciprocal\ flattening: 1/f = 298{,}257223563$$

$$Flatness: f = \frac{a-b}{a} = 0.00335281$$

$$Semiminor\ axis: b = a(1-f) = 6356752{,}314\ m$$

$$Eccentricity: e = \sqrt{f(2-f)} = 0{,}08181919$$

In GPS applications the transformation between reference frames is very much involved. ECEF coordinates can be found by the following formula if the geodetic coordinates are known

$$x = (N+h)\,cos(\lambda)\,cos(\emptyset)$$

$$y = (N+h)\,cos(\lambda)\,sin(\emptyset)$$

$$z = [N(1-e^2)+h]sin(\lambda)$$

Where N is the length of the normal to the ellipsoid and is defined as

$$N = a/(1-e^2 sin^2\emptyset)^{1/2}$$

Geodetic coordinates can be found by the following inverse formulas

$$\emptyset = \text{atan}[\frac{z}{\sqrt{x^2 + y^2}}]$$

$$\lambda = \text{atan}\left[\frac{y}{x}\right]$$

$$h = \sqrt{x^2 + y^2}\, cos\emptyset + z\, sin\emptyset - R$$

Appendix D

Real time data collection

High-end IMU

```
# Week        ToW (s)       Lat (deg)        Lon (deg)    Hght (m) vN
(m/s) vE (m/s) vD (m/s)    Roll(d)    Pitch(d)     Head(d)  sN (m)  sE
(m)  sH (m)  sR (m)  sP (m) sHd (m)  #S    PDOP    rN (m)    rE (m)
rH (m)
#-------------------------------------------------------------------
-------------------------------------------------------------------
-------------------------------------------------------------------
--------
 1652  203681.000000   59.665397006    10.777538179   136.4650
0.6999   1.5033   0.0352   -0.34473   -0.98545   66.27961   0.033
0.044   0.049   0.001   0.001   0.004  14     1.4     0.015
0.014     0.027
 1652  203682.000000   59.665406431    10.777566941   136.4831
1.0224   1.7557  -0.0482    2.01269   -1.25585   59.42447   0.033
0.044   0.049   0.001   0.001   0.004  15     1.4     0.021
0.014     0.041
```

Low-end IMU

```
TSTAMP AX AY AZ GX GY GZ
File 48D764423632-2011-09-06-06-19.bin opened OK
69292620 -199 -2 971 166 315 -227
69292640 -207 15 977 105 -507 113
69292660 -201 -6 962 253 -577 -262
69292680 -202 -5 964 385 -358 113
```

GPS

```
TSTAMP YYYY-MM-DD HH:MM:SEC lat lon alt speed heading est_hor_err
est_vert_err #sat_in_fix HDOP SBAS_applied
File 48D764423632-2011-09-06-06-19.bin opened OK
69986225 2011-9-6 8:34:26 59.665352 10.777636 94 1.79 55 0.04 0.01 8
0.80 0
69987235 2011-9-6 8:34:27 59.665363 10.777658 94 2.00 40 0.04 0.01 8
0.80 0
```

Appendix E

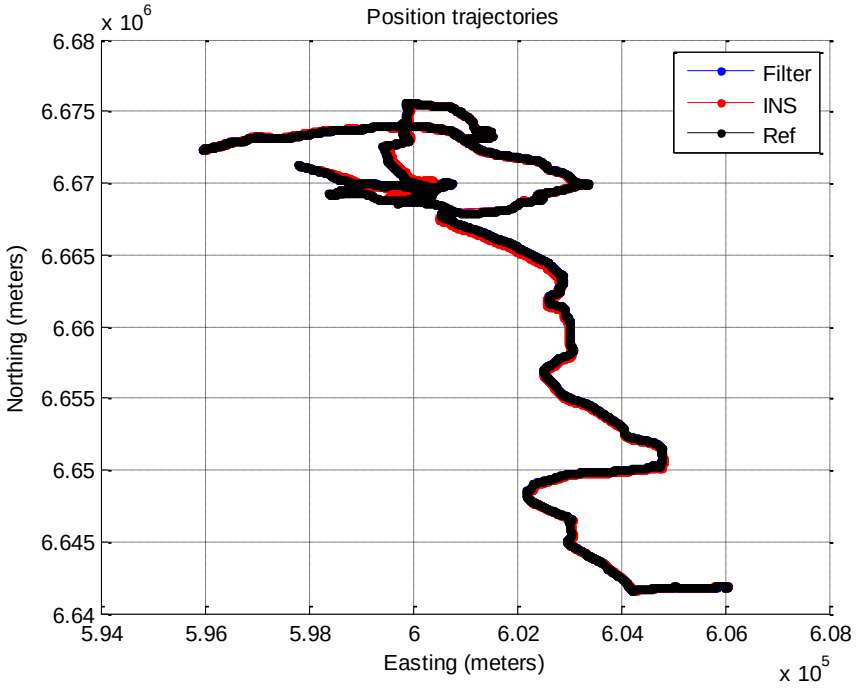
Position trajectories
x 10^6
6.68
6.675
6.67
6.665
6.66
6.655
6.65
6.645
6.64
Northing (meters)
Filter
INS
Ref
5.94
5.96
5.98
6
6.02
6.04
6.06
6.08
Easting (meters)
x 10^5

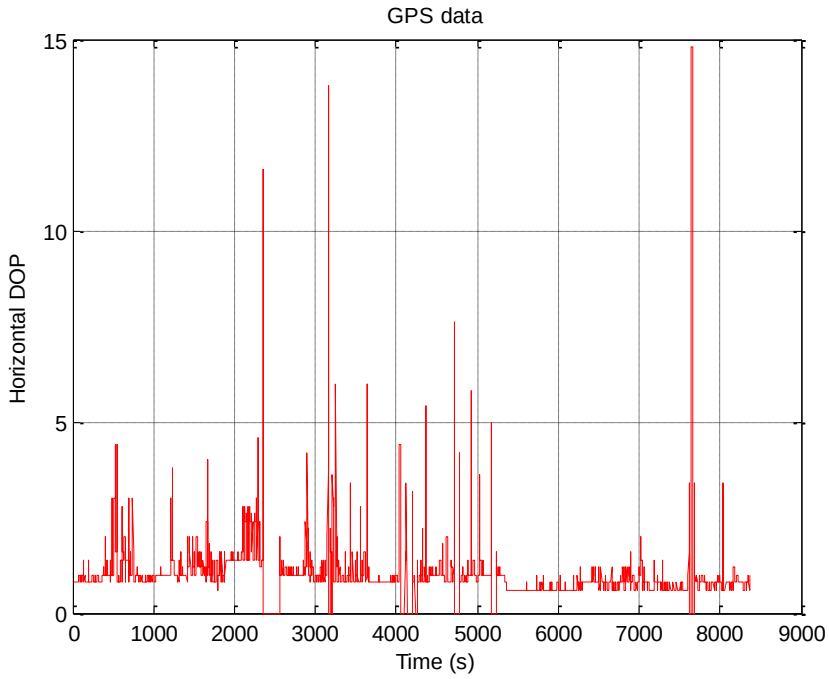
GPS data
15
10
5
0
Horizontal DOP
0
1000
2000
3000
4000
5000
6000
7000
8000
9000
Time (s)

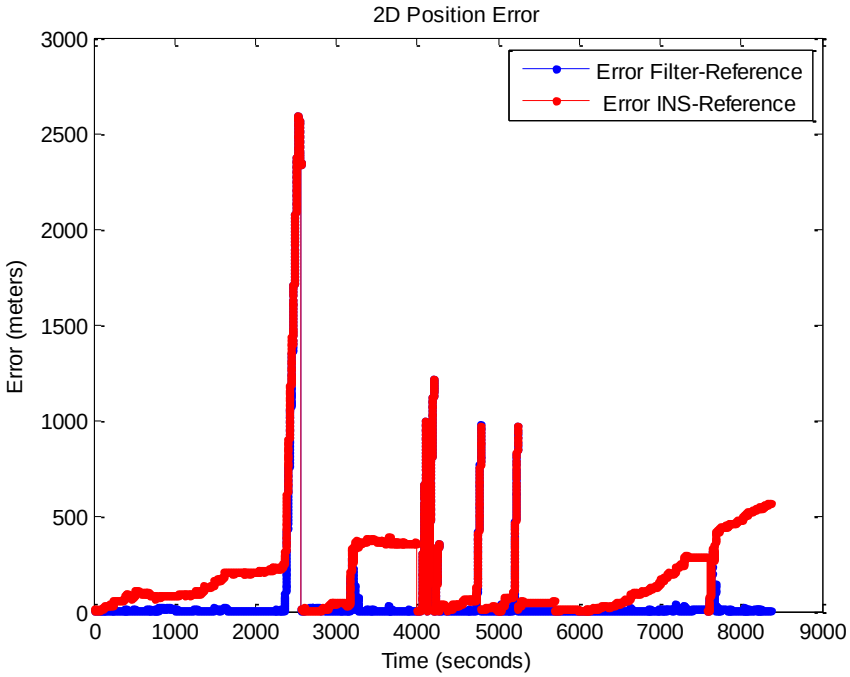
2D Position Error
Error Filter-Reference
Error INS-Reference
Error (meters)
Time (seconds)
3000
2500
2000
1500
1000
500
0
0
1000
2000
3000
4000
5000
6000
7000
8000
9000

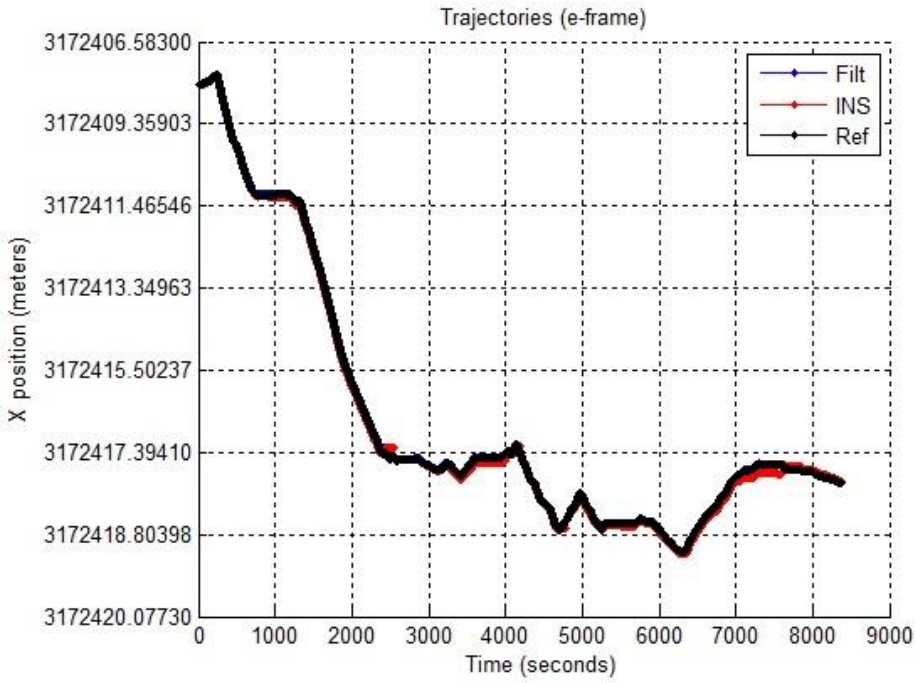
Trajectories (e-frame)
Filt
INS
Ref
X position (meters)
Time (seconds)
3172406.58300
3172409.35903
3172411.46546
3172413.34963
3172415.50237
3172417.39410
3172418.80398
3172420.07730
0
1000
2000
3000
4000
5000
6000
7000
8000
9000

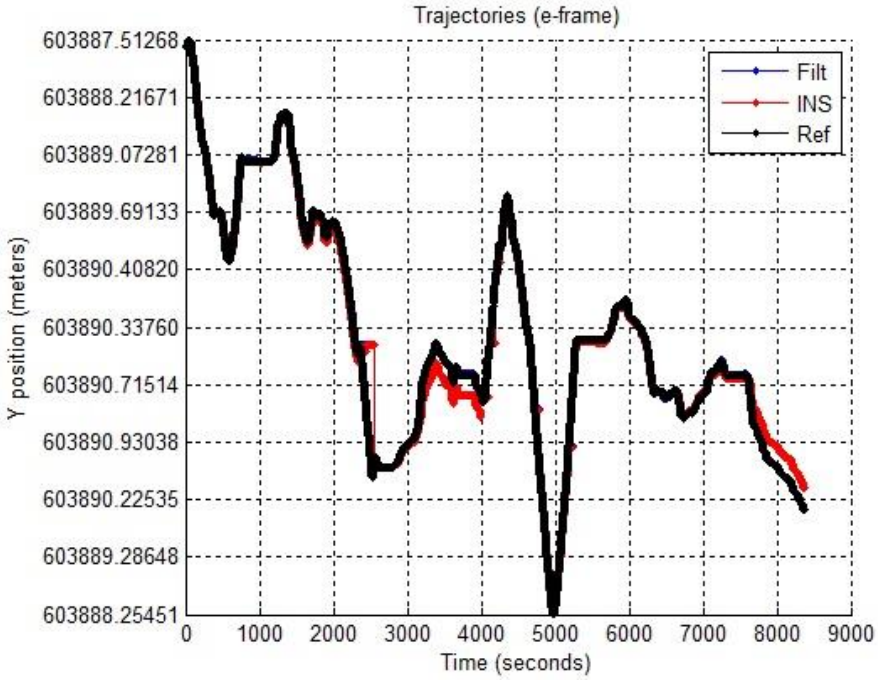
Trajectories (e-frame)
Filt
INS
Ref
Y position (meters)
603887.51268
603888.21671
603889.07281
603889.69133
603890.40820
603890.33760
603890.71514
603890.93038
603890.22535
603889.28648
603888.25451
0
1000
2000
3000
4000
5000
6000
7000
8000
9000
Time (seconds)

Appendix F

Dokumentasjon og koordinater for GNSS-/INS-målebil

Are Jo Næss
Universitet for Miljø og Biovitenskap
12. oktober 2011

Programvare: PhotoModeler Pro 5.2.3
Enhet i prosjektet: millimeter

Koordinatene er gitt i samme koordinatsystem som GNSS/INS-ramma som ble beskrevet i «Dokumentasjon og koordinater for GPS- og INS-ramme 18.03.2009» av Ivar Maalen-Johansen. Punkt-Id 1-3 er kjentpunkt fra GNSS/INS-ramma. Punkt 5 og 6 er kodemottakere. Resterende punkter er kun hjelpepunkt/sammenbindingspunkt brukt til å orientere bildene.

Tabell 1: Målte punkt

		Koordinater - mm			**Presisjon - mm**		
Id	**Navn**	**X**	**Y**	**Z**	**X**	**Y**	**Z**
1	**(10) RecA**	**86.7**	**783.4**	**-88.8**	**1.7**	**0.5**	**0.5**
2	**(11) RecC**	**1380.7**	**783.2**	**-95.7**	**0.6**	**0.5**	**0.6**
3	**(12) RecB**	**1381.0**	**88.4**	**-89.9**	**0.6**	**0.6**	**0.5**
5	**Q-free - mottaker**	**2397.6**	**558.8**	**726.3**	**0.7**	**0.3**	**0.4**
6	**Håndholdt mottaker m/EGNOS**	**2327.7**	**501.1**	**577.0**	**0.6**	**0.3**	**0.4**
4	-	2400.4	528.1	726.4	0.7	0.3	0.4
7	-	2308.0	1154.0	642.1	0.6	0.9	0.4
8	-	1825.8	1032.2	255.9	0.4	0.8	0.3
9	-	-163.4	1256.2	752.0	2.0	0.8	0.9
10	-	34.0	1252.6	682.5	1.8	0.8	0.7
12	-	175.7	123.0	-80.6	1.5	0.5	0.5
13	-	1864.2	-202.5	299.8	0.4	0.9	0.3
15	-	-3578.7	722.3	602.1	3.7	0.7	1.0
16	-	-3586.2	362.8	597.4	3.7	0.8	1.0
18	-	-3561.4	-464.4	988.4	4.7	1.1	1.4
19	-	-3551.0	1365.8	567.8	8.1	0.8	1.6
21	-	2084.8	412.8	389.8	0.4	0.3	0.2
22	-	2419.8	-275.4	735.5	0.8	1.0	0.5
23	-	-2541.8	-1596.9	-130.4	4.8	2.4	0.7

Figur 1: Skjermdump fra PhotoModeler

Kamerakalibrering - konstanter beregnet:

```
Camera1: Canon D450 JGG
   Focal Length                          K1 - radial distortion 1
      Value: 18.542617 mm                   Value: 5.318e-004
      Deviation: Focal: 0.002 mm            Deviation: K1: 2.2e-006
   Xp - principal point x                K2 - radial distortion 2
      Value: 11.194518 mm                   Value: -1.187e-006
      Deviation: Xp: 0.003 mm               Deviation: K2: 2.0e-008
   Yp - principal point y                K3 - radial distortion 3
      Value: 7.313061 mm                    Value: 0.000e+000
      Deviation: Yp: 0.003 mm            P1 - decentering distortion 1
   Fw - format width                        Value: -2.998e-005
      Value: 22.254661 mm                   Deviation: P1: 2.2e-006
      Deviation: Fw: 8.7e-004 mm         P2 - decentering distortion 2
   Fh - format height                       Value: -2.248e-005
      Value: 14.833600 mm                   Deviation: P2: 2.3e-006
```

Appendix G

Matlab Code

```
% Navigation frame: e-frame

% Inital conditions

close all
clear all

load imu.log;
load pos.log;
load obu_ref.inp

initial_roll = obu_ref(1,9)*pi/180;
initial_pitch = obu_ref(1,10)*pi/180;
initial_yaw = obu_ref(1,11)*pi/180;

time_imu = 1:1/50:8369;
time_gps = 1:1:8369;

lat = pi/180*pos(1,4);
lon = pi/180*pos(1,5);

%% Memory allocation
pos_ecef = zeros(length(pos),3);
ref_ecef = zeros(length(pos),3);
pos_neu= zeros(length(pos),3);
error_ecef = zeros(length(pos),1);
error_Filter_Ref=zeros(length(pos),1);
error_INS_Ref=zeros(length(pos),1);
error_g = zeros(length(pos),3);
error = zeros(length(pos),1);
NE_filt = zeros(length(pos),2);
NE_ref = zeros(length(pos),2);
NE_ins = zeros(length(time_imu),2);
%%

h = pos(1,6);
az = pos(:,8)*pi/180;
v = pos(:,7);    % m/s

% System conditions
dt = 1;
t=1/50;                          % time interval
% R_e=6371000;                    % Earth radius (m)
a = 6378137;
b = 6356752.314;
% a = R_e;
% b = R_e;
oie_e=[0;0;7292115e-11];    %  Earth rotation (rad/s)
geb_g=[0;0;9.80665];          % Gravity vector
position_update = 1;         % Flag for position update at points where GPS
signals are back

% Convertion of GPS position to ECEF
```

```
for i = 1:length(pos)
    [X0,Y0,Z0]=geod2ECEF(a,b,pi/180*pos(i,4),pi/180*pos(i,5),h);
    pos_ecef(i,1) = X0;
    pos_ecef(i,2) = Y0;
    pos_ecef(i,3) = Z0;

[X0,Y0,Z0]=geod2ECEF(a,b,pi/180*obu_ref(i,3),pi/180*obu_ref(i,4),obu_ref(i,5))
;
    ref_ecef(i,1) = X0;
    ref_ecef(i,2) = Y0;
    ref_ecef(i,3) = Z0;

end
%Initializations for Kalman filering
%%
P = [64 0 0 0 0;0 16 0 0 0;0 0 9 0 0;0 0 0 9 0;0 0 0 0 9];
P = kron(eye(3),P);%eye(6);% Initial Covariance
 sv = 0.8;% White noise spectral density
 sw = 0.005;
 sa = 0.01;
q_pv = sv^2*[1/3*dt^3 1/2*dt^2;1/2*dt^2 dt];
q_gyro = sw^2*[1/3*dt^3 1/2*dt^2;1/2*dt^2 dt];
q_acc = sa^2*[1/3*dt^3 1/2*dt^2;1/2*dt^2 dt];
Q = [[q_pv] zeros(2,2) zeros(2,2);zeros(2,2) q_gyro zeros(2,2);zeros(2,2)
zeros(2,2) q_acc];
Q = kron(eye(3),Q); % Scaling of process noise matrix
H = [1 0 0 0 0;0 0 0 1 0;0 0 0 0 1];
H = kron(eye(3),H); %Design Matrix
[n,e] = size(H);               % Length of state vector
R = diag([1 0.03^2 0.03^2]); % Measurement variance matrix
R = kron(eye(3),R);
phi = [1 dt 0 0 0;0 1 0 0 0;0 0 1 dt 0;0 0 0 1 0;0 0 0 0 1];
phi = kron(eye(3),phi);

%%

% Gyro observations
% n = length(pos)*50; % Pos.log has a lesser length
gyrox=pi/180*1e-3*imu(:,5);
gyroy=pi/180*1e-3*imu(:,6);
gyroz=pi/180*1e-3*imu(:,7);
time = 1e-3*(imu(:,1)-imu(1,1));


% Accelerometer observations
accx=imu(:,2)*9.8*1e-3;
accy=imu(:,3)*9.8*1e-3;
accz=imu(:,4)*9.8*1e-3;

%% Memory allocation for saving data
INS = zeros(length(time_imu),3); %position in g-frame Without filter
(integrated)
filt_states = zeros(length(pos),12); % Filtered position
RMS = zeros(length(pos),1);

%%
```

```
INS(1,:)=[pos_ecef(1,1),pos_ecef(1,2),pos_ecef(1,3)]; % position (g-frame)
X_INS = pos_ecef(1,1);
Y_INS = pos_ecef(1,2);
Z_INS = pos_ecef(1,3);

Xr =
[pos_ecef(1,1);0;initial_roll;0;pos_ecef(1,2);0;initial_pitch;0;pos_ecef(1,3);
0;initial_yaw;0];
j_inc = 0;

for i = 1:418400

    j = floor(i/50)+1;
    j_it=j-j_inc;
    interval1 = 2450:2556;
    interval2 = 4000:4107;
    interval3 = 4100:4199;
    interval4 = 4200:4262;

    oib_b=[-gyrox(i);-gyroy(i);gyroz(i)];
    fib_b=[accx(i);accy(i);accz(i)];
    veb_b = [v(j); 0 ;0];

 % Compute Cb_e

  Ce_g=[-sin(lat)*cos(lon) -sin(lat)*sin(lon) cos(lat);
      -sin(lon) cos(lon) 0;
      -cos(lat)*cos(lon) -cos(lat)*sin(lon) -sin(lat)];
  Cb_g=Rz(az(j))*Ry(0)*Rx(0);

  Cb_e=Ce_g'*Cb_g;

  veb_e=Cb_e*veb_b;

  % Convert geod2ECEF
  [X0,Y0,Z0]=geod2ECEF(a,b,lat,lon,h);


  %Initial state vector
  if (ismember(j,interval1)||ismember(j,interval2)|| ismember(j,interval3) ||
ismember(j,interval4)|| j == 2557 || j == 4106 || j==4199 || j == 4783 || j
==5233 || j==5685 || j ==7581|| j ==7608 )
       Xr(1) = pos_ecef(j,1);
       Xr(5) = pos_ecef(j,2);
       Xr(9) = pos_ecef(j,3);
      X_INS = pos_ecef(j,1);
      Y_INS = pos_ecef(j,2);
      Z_INS = pos_ecef(j,3);
  end

   if(j_it)
   Xr = phi*Xr;     %state estimation vector update
   P = phi*P*phi'+Q;    %state covariance prediction
```

```
    end
    % Compute gyro rate
    oeb_b=oib_b-Cb_e'*oie_e;
    Oeb_b=crossm(oeb_b);

    % Compute Cb_e_dot

    Cb_e_dot=Cb_e*Oeb_b;

    % Update Cb_e
    Cb_e_hat=Cb_e+Cb_e_dot*t;

    % Normalize
    Cb_e=normalize(Cb_e);

    % Compute Earth Rotation
    Oie_e=crossm(oie_e);

    % Compute acceleration in e-frame
    aeb_e=Cb_e_hat*fib_b-(2*Oie_e)*veb_e+Ce_g'*geb_g;

    % Compute velocity in e-frame
    veb_e=Cb_e_hat*veb_b+aeb_e*t;
    %veb_e=veb_e+aeb_e*t;
    Xr(2) = veb_e(1);
    Xr(6) = veb_e(2);
    Xr(10) = veb_e(3);
    % Compute pos increment in e-frame
    dreb_e=veb_e*t;


    ve_g = Ce_g*veb_e;

    %% Saving data
    X_INS = X_INS+dreb_e(1);
    Y_INS = Y_INS+dreb_e(2);
    Z_INS = Z_INS+dreb_e(3);

    INS(i+1,:)=[X_INS,Y_INS,Z_INS]; % position (g-frame)

    %% Kalman Filter




     % Convert ECEF2geod
     [lat,lon,h]=ECEF2geod(a,b,INS(i+1,1),INS(i+1,2),INS(i+1,3));
     [N_ins,E_ins] = geod2NE(a,lat,lon);
     NE_ins(i,1) = N_ins;
     NE_ins(i,2) = E_ins;

%% kalman update
 if(j_it)
```

```
     oib_b0 = Cb_e_hat'*oie_e + Cb_e_hat*crossm([Xr(3) Xr(7)
Xr(11)]')*oie_e+[Xr(4);Xr(8);Xr(12)];
     Xt =
[pos_ecef(j,1);oib_b(1);pos_ecef(j,2);oib_b(2);pos_ecef(j,3);oib_b(3)]; %
State observation vector (e-frame)

  K = P*H'/(H*P*H'+R); % Kalman gain
  z = [Xt(1)-Xr(1);Xt(2)-oib_b0(1);Xt(3)-Xr(5);Xt(4)-oib_b0(2);Xt(5)-
Xr(9);Xt(6)-oib_b0(3)];%H*Xt; %Observation model
  Xr = Xr+K*z;%(z-H*Xr);%Update state estimate
  P=(eye(e)-K*H)*P*(eye(e)-K*H)'+K*R*K'; % Covariance estimate update
  filt_states(j,:) = Xr;    % Position in e-frame
    [lat0,lon0,h0] =
ECEF2geod(a,b,filt_states(j,1),filt_states(j,5),filt_states(j,9));
  [N_filt,E_filt] = geod2NE(a,lat0,lon0);
  NE_filt(j,1) = N_filt;
  NE_filt(j,2) = E_filt;
  [N_ref,E_ref] = geod2NE(a,obu_ref(j,3)*pi/180,obu_ref(j,4)*pi/180);
  NE_ref(j,1) = N_ref;
  NE_ref(j,2) = E_ref;
  error_Filter_Ref(j) = sqrt((N_filt-N_ref)^2+(E_filt-E_ref)^2);

  error_INS_Ref(j) = sqrt((N_ins-N_ref)^2+(E_ins-E_ref)^2);

 end
  j_inc = j;
end

figure(1)
hold on
plot(time_gps,filt_states(1:end-1,1),'.-b');grid;shg
plot(time_imu(1:end-1),INS(1:end-1,1),'.-r');grid;shg
plot(time_gps,ref_ecef(1:end-1,1),'.-k');grid;shg
legend('Filt','INS','Ref')
xlabel('Time (seconds)');
ylabel('North position');

figure(2)
hold on
plot(time_gps,filt_states(1:end-1,5),'.-b');grid;shg
plot(time_imu(1:end-1),INS(1:end-1,2),'.-r');grid;shg
plot(time_gps,ref_ecef(1:end-1,2),'.-k');grid;shg
legend('Filt','INS','Ref')
xlabel('Time (seconds)');
ylabel('East position');

figure(3)
plot(time_gps,error_Filter_Ref(1:end-1),'.-');grid;shg
% hold on;plot(time_gps,error_INS_Ref(1:end-1),'.-r');grid;shg
% legend('Error Filter-Reference',' Error INS-Reference')
legend('Error Filter-Reference')
xlabel('Time (seconds)');
ylabel('Error (meters)');

figure(4)
hold on
```

```
plot(NE_filt(1:end-1,1),NE_filt(1:end-1,2),'.-b');grid;shg
plot(NE_ins(1:end-1,1),NE_ins(1:end-1,2),'.-r');grid;shg
plot(NE_ref(1:end-1,1),NE_ref(1:end-1,2),'.-k');grid;shg
legend('Filter','INS','Ref')
title('Trajectories')
xlabel('Northing (meters)');
ylabel('Easting (meters)');


figure(5)
hold on
plot(time_gps,NE_filt(1:end-1,1),'.-b')
plot(time_imu,NE_ins(:,1),'.-r')
plot(time_gps,NE_ref(1:end-1,1),'.-k')
legend('Filter','INS','Ref')
title('Northing')

figure(6)
hold on
plot(time_gps,NE_filt(1:end-1,2),'.-b')
plot(time_imu,NE_ins(:,2),'.-r')
plot(time_gps,NE_ref(1:end-1,2),'.-k')
legend('Filter','INS','Ref')
title('Easting')

figure(7)
hold on
plot(NE_filt(1:end-1,2),NE_filt(1:end-1,1),'.-b');grid;shg
plot(NE_ins(1:end-1,2),NE_ins(1:end-1,1),'.-r');grid;shg
plot(NE_ref(1:end-1,2),NE_ref(1:end-1,1),'.-k');grid;shg
legend('Filter','INS','Ref')
title('Position trajectories')
xlabel('Easting (meters)');
ylabel('Northing (meters)');

figure(8)
hold on
plot3(time_gps,NE_filt(1:end-1,1),NE_filt(1:end-1,2),'.-b')
plot3(time_imu(1:end-1),NE_ins(1:end-1,1),NE_ins(1:end-1,2),'.-r')
plot3(time_gps,NE_ref(1:end-1,1),NE_ref(1:end-1,2),'.-k')
legend('Filter','INS','Ref')
title('Trajectories')
xlabel('Northing (meters)');
ylabel('Easting (meters)');

% Number of Satellites vs time.
x = obu_ref(:,18); % No. of satellites available (Reference)
y = pos(:,11); % No. of satellites available (GPS)
EH = pos(:,9); % East horizontal error.
EV = pos(:,10); % East vertical error.


HDOP = pos(:,12);
PDOP = obu_ref(:,19);
```

```
figure(9)
plot(time_gps,x(1:end-1),'-b')
title('Reference data')
xlabel('Time (seconds)');
ylabel('Number of Satellites');
grid on

figure(10)
plot(time_gps,y(1:end-1),'-b')
title('GPS data')
xlabel('Time (seconds)');
ylabel('Number of Satellites');
grid on

figure(11)
plot(time_gps,HDOP(1:end-1),'-r')
title('GPS data')
xlabel('Time (s)');
ylabel('Horizontal DOP');
grid on

figure(12)
plot(time_gps,PDOP(1:end-1),'-r')
title('Reference data')
xlabel('Time (s)');
ylabel('Position DOP');
grid on

figure(13)
plot(time_gps,x(1:end-1),'-b')
hold on
plot(time_gps,y(1:end-1),'-r')
legend('Reference','GPS')
title('Available Satellites')
xlabel('Time (seconds)');
ylabel('Number of Satellites');
grid on

figure(14)
hold on
plot(time_gps,filt_states(1:end-1,1),'.-');grid;shg
set(gca,'YTickLabel',sprintf('%4.5f|',filt_states(1:end-1,1)))
plot(time_imu(1:end-1),INS(1:end-1,1),'.-r');grid;shg
plot(time_gps,ref_ecef(1:end-1,1),'.-k');grid;shg
legend('Filt','INS','Ref')

figure(15)
hold on
plot(time_gps,filt_states(1:end-1,5),'.-b');grid;shg
set(gca,'YTickLabel',sprintf('%4.5f|',filt_states(1:end-1,5)))
plot(time_imu(1:end-1),INS(1:end-1,2),'.-r');grid;shg
plot(time_gps,ref_ecef(1:end-1,2),'.-k');grid;shg
legend('Filt','INS','Ref')

figure(16)
plot(time_gps,error_Filter_Ref(1:end-1),'.-');grid;shg
```

```
hold on;plot(time_gps,error_INS_Ref(1:end-1),'.-r');grid;shg
legend('Error Filter-Reference',' Error INS-Reference')

figure(17)
hold on
plot(NE_filt(1:end-1,1),NE_filt(1:end-1,2),'.-b')
set(gca,'YTickLabel',sprintf('%4.5f|',NE_filt(1:end-1,2)))
plot(NE_ins(1:end-1,1),NE_ins(1:end-1,2),'.-r')
plot(NE_ref(1:end-1,1),NE_ref(1:end-1,2),'.-k')
legend('Filter','INS','Ref')
xlabel('North (meters)');
ylabel('East (meters)');
```